J. Ulman

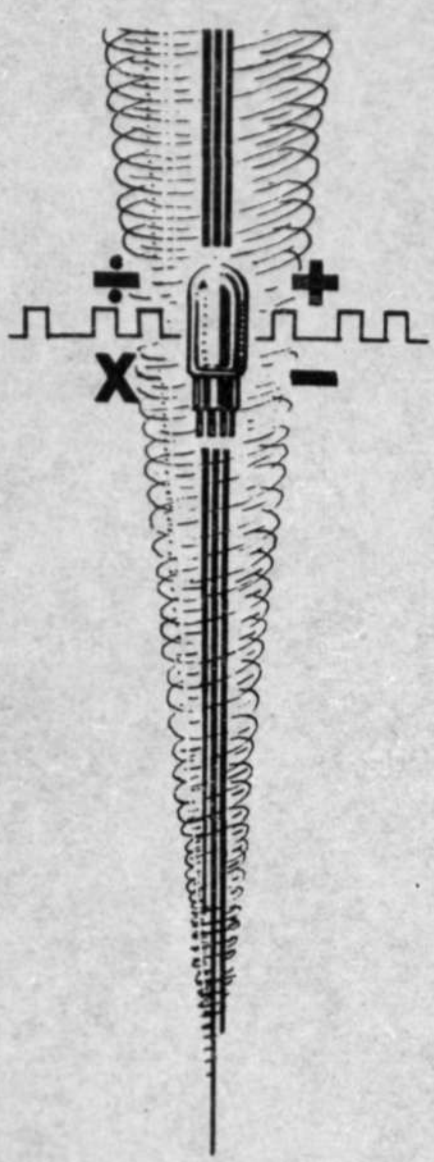

PROJECT WHIRLWIND

Contract N5ori60

REPORT R-192

A COINCIDENT-CURRENT MAGNETIC MEMORY UNIT

SEPTEMBER 8, 1950

SERVOMECHANISMS LABORATORY
MASSACHUSETTS INSTITUTE OF TECHNOLOGY

Copy 63

PROJECT WHIRLWIND

Report R-192

A COINCIDENT-CURRENT MAGNETIC MEMORY UNIT

Submitted to the

OFFICE OF NAVAL RESEARCH

Under Contract N5ori60

Project NR-048-097

Report by
William N. Papian

SERVOMECHANISMS LABORATORY
MASSACHUSETTS INSTITUTE OF TECHNOLOGY
Cambridge 39, Massachusetts
Project DIC 6345

September 8, 1950
(Thesis Date August 31, 1950)

FOREWORD

Because it presents information of general interest, this thesis report, which has had only limited distribution, is being issued as a Project Whirlwind R-series report.

Any new data-storage development which suggests promise of increased reliability and decreased bulk is of immediate interest to the builders of a large scale digital computer such as Whirlwind. The use of rectangular-loop magnetic cores in a multi-dimensional storage scheme, as suggested by Jay W. Forrester, Director of Project Whirlwind, holds such promise. This investigation was, therefore, undertaken.

Mr. Forrester supervised the thesis work. Invaluable aid was received from members of the mathematics, logical-design, electronic-circuits, drafting, reports, and clerical sections of the organization. The author is also grateful for the cooperation of Mr. John H. Crede and the Allegheny Ludlum Steel Corporation, who supplied the bulk of the metallic cores in the experimental work.

TABLE OF CONTENTS

Page

ABSTRACT

A small, toroidal, ferromagnetic core whose B-H characteristic is properly "rectangular" in shape may be made to operate so that its flux polarity reverses only when the right combination of two or three magnetizing coils are coincidentally excited. The core may then be used as a coincident-current binary memory device which might be assembled, with many others, into a two- or three-dimensional memory system. Selection within such a system would be accomplished by means of physical-line switching along the two or three space coordinates.

The response times of rectangular-loop cores are found to vary over an extremely large range. To a first approximation, eddy-current shielding accounts for these response times, which range from tenths of a second for some metallic cores to less than a microsecond for some ferritic cores.

Information-retention ratios and signal ratios are defined and are used to assess the ability of a core to operate as a coincident-current memory unit. A test setup which makes it possible to obtain these ratios for different sets of operating conditions is devised and used on a number of cores. Selected results are presented and discussed relative to the pertinent hysteresis-loop shapes.

The problem is bracketed on the one hand by a metallic core (Allegheny Ludlum's MTS 4382) which has excellent signal ratios and a 20-microseconds response time, and on the other hand, by a ferritic core (Ferramic 34-A F109 b.o.) which has only fair signal ratios and a 1/2-microsecond response time.

Further development work should be aimed in two directions: toward improving materials to reduce eddy currents and increase hysteresis-loop rectangularity, and toward uncovering and solving the problems associated with assembling large numbers of these cores into a high-speed memory system.

CHAPTER I

INTRODUCTION

A. Background

Data storage is one of the functions in modern computer, control, and communications systems. It is a major function in electronic digital computers, whose designs have developed, to a significant degree, around the limitations and potentialities of chosen storage media.

The storage medium now being incorporated into the computer at Project Whirlwind is a cathode-ray type of electrostatic storage tube. The data are in the form of binary digits which are stored as spots of electric charge on a plane dielectric surface within the tube. A particular spot is "selected" by aiming the cathode ray; two space coordinates in the form of vertical and horizontal deflection voltages determine the position of the spot. "Writing" or "reading" the spot is a second step accomplished by bringing the tube elements up to the proper voltage levels and turning on the cathode ray.

This type of tube uses only two space coordinates in the selection step of the data storage process. The extension to three or more space coordinates would result in a reduction of both the storage medium bulk[1] and the number of subdivisions along each coordinate axis for a given storage capacity.

---

1. Superscripts refer to numbered items in the bibliography.

Position along a coordinate axis is determined, in the cathode-ray type of storage tube, by the level of a deflection voltage. A more discrete determination of coordinate position in a storage medium would be obtainable by the selection of one of a number of physical lines.

Research toward development of a three-dimensional storage scheme wherein discrete space-coordinates are used in the selection process was under way at Project Whirlwind early in 1947.[2] One of the media investigated was the low-pressure-gas glow-discharge tube. It, however, proved infeasible for practical reasons.

Work started again in the spring of 1949. The development of small ferromagnetic cores with rectangular hysteresis loops reopened interest in the problem. It seemed possible that suitable cores could be assembled into a three-dimensional storage array, with a selection scheme involving three single-pole line-switching mechanisms.[1] This thesis is part of that work; it is concerned primarily with the individual core.

The following sections of this chapter explain the elements of this three-dimensional storage scheme and indicate some of the general requirements on the core. The detailed discussion of the individual core starts in Chapter II.

B. Basic Operation of the Individual Core

Briefly, a small core made of a "hard" magnetic material may be magnetized in one direction or the other, and left that way. This bi-stability, like that of a two-position relay, may be used to express the two digits of the binary system, ZERO or ONE. A number may be stored, or written, by sending a current pulse through a magnetizing coil on the core. Reversing the polarity of this current reverses the core's magnetization.

The binary number in the core, represented by the core's flux direction, may be sensed, or read, by observing the voltage induced in a sensing coil when the magnetizing coil carries a current pulse of fixed arbitrary polarity and magnetizing amplitude. Relatively large signal voltages will be induced if the core flux direction is reversed by the read pulse, small ones if it is not. This basic scheme is approximately the one investigated by the Computation Laboratory of Harvard University.[3]

A core with a sufficiently rectangular hysteresis loop may be used in the following scheme for utilizing line-switching along space coordinates in the selection step of the storage process. Figure 1(a) is a schematic representation of such a core. Windings A and B are magnetizing, or selecting, coils; S is a sensing coil. Assume that a hysteresis loop of the core is as shown in Figure 1(b), and that, at the start, the operating point is at the lower stable position $-B_R$.

The application of a magnetizing force of amplitude $H_M/2$ moves the operating point to x, resulting in a very small change in flux density B; return to H = 0, which occurs at the end of the $H_M/2$ pulse, moves the operating point to $-B_N$, a point not far removed from $-B_R$.

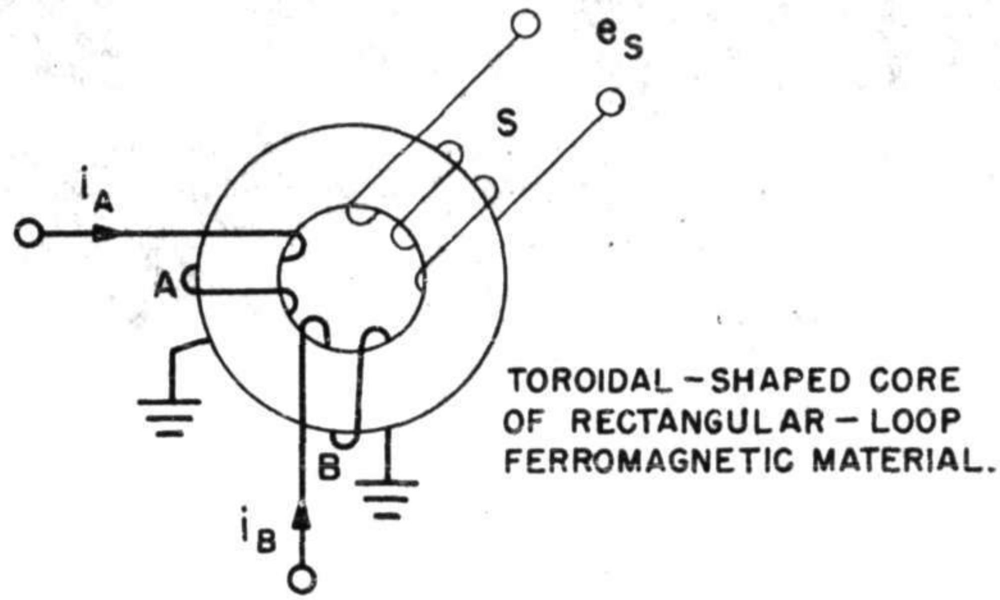

(a) A TWO-CURRENT-COINCIDENCE MEMORY UNIT

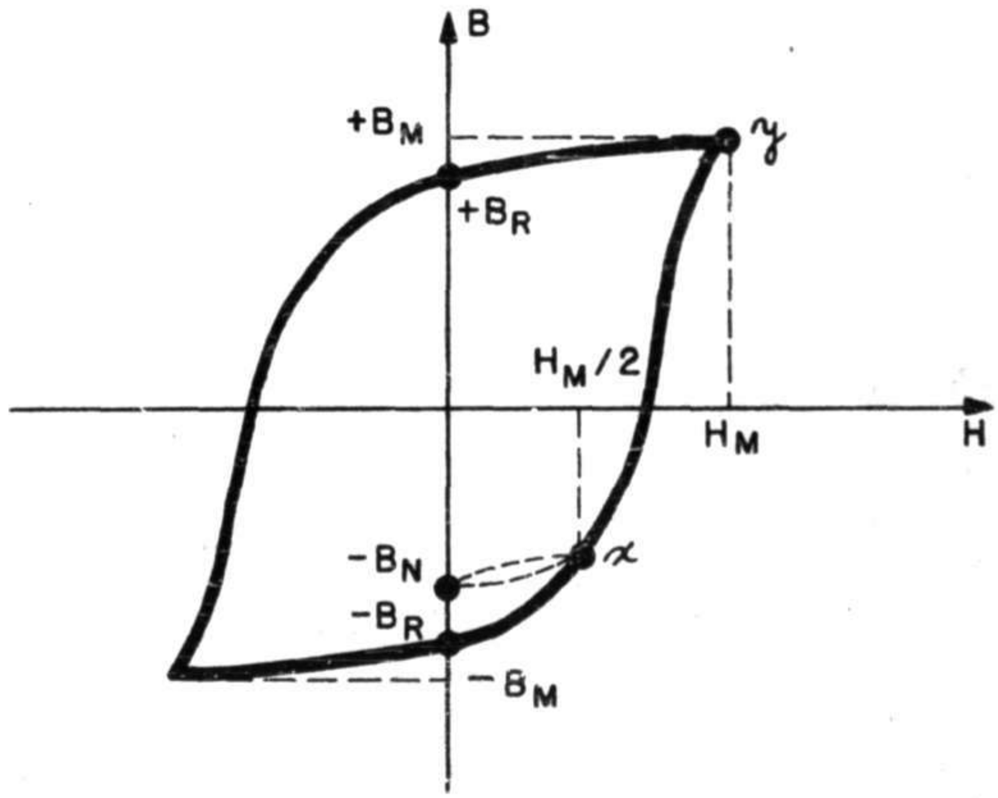

(b) PATHS OF OPERATION OF A MAGNETIC MEMORY UNIT

A-35232P

FIG. 1

The result for the application and removal of the full H_M is quite different; the operating point moves to y, and then to $+B_R$. The core reverses its magnetization upon application of H_M; in the process there is a large change of flux density B, with a correspondingly large pulse induced in the signal coil.

If the currents i_A and i_B are made equal and of such an amplitude that they correspond to values of magnetizing force equal to $H_M/2$ each, then the magnetization of the core can be changed from $-B_R$ to $+B_R$ only by the addition, or coincidence, of i_A and i_B. The development of a relatively large signal pulse would, therefore, depend on such coincidence. Reversing the current direction reverses the procedure.

(It is apparent that forms of noise and instability result from the minor hysteresis loops travelled when magnetizing forces less than H_M are applied and removed. These and other factors make desirable a very high degree of hysteresis-loop rectangularity and a relatively high coercivity in the core material. Quasi-static operation has been assumed; obviously, the frequency with which operations may occur will be limited by losses, eddy-current shielding, and other factors. Later chapters discuss some of these problems in detail.)

One simple criterion for the shape of the B-H loop may be derived from the idealized loop drawn in Figure 2. If the values of H for which the loop turns a sharp corner into a new region are called H_1 and H_2 as shown, then coincident-current operation is assured when the following hold true:

$$H_M > H_2 \qquad (1)$$

$$\frac{H_M}{2} < H_1. \qquad (2)$$

These may be combined to give the coincident-current criterion:

$$2H_1 > H_M > H_2, \qquad (3)$$

or: $H_2 < 2H_1$.

C. Two- and Three-Dimensional Storage

If now, for example, nine of these cores are arranged in a two-dimensional array as in Figure 3, and currents of magnitude $I_M/2$ are caused to flow in selected lines y_2 and x_3 as shown, core F is the only core in the array which has the full magnetizing force H_M impressed. Cores D, E, C and I have $H_M/2$ impressed; the rest have no impressed magnetizing force. The only core, therefore, whose magnetization can be significantly affected is the one at the junction of the selected lines. The output signal may be taken, after suitable mixing, from the coils marked S which are all connected in common.

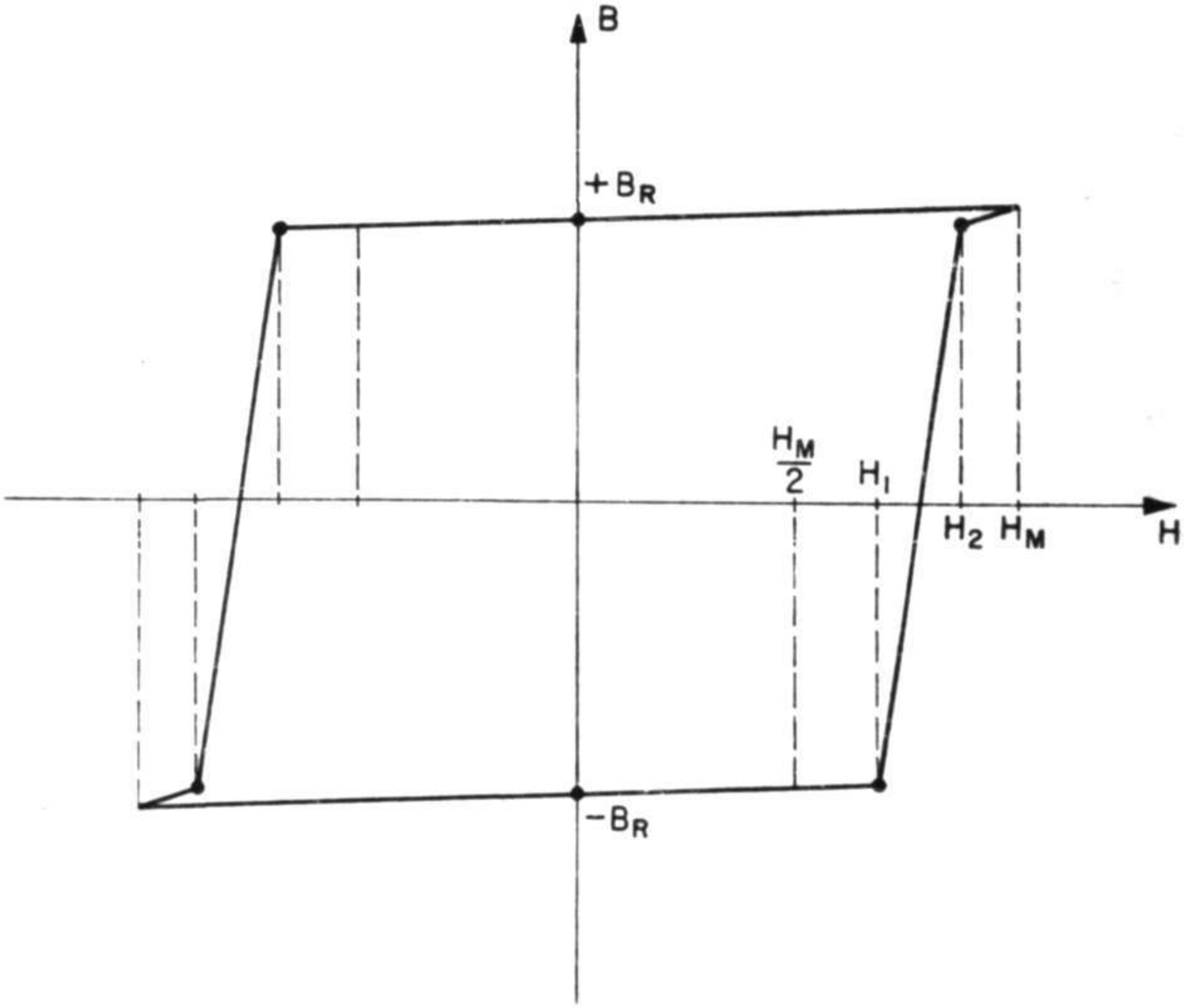

AN IDEALIZATION OF A B-H LOOP

A-36009

FIG. 2

A-35792

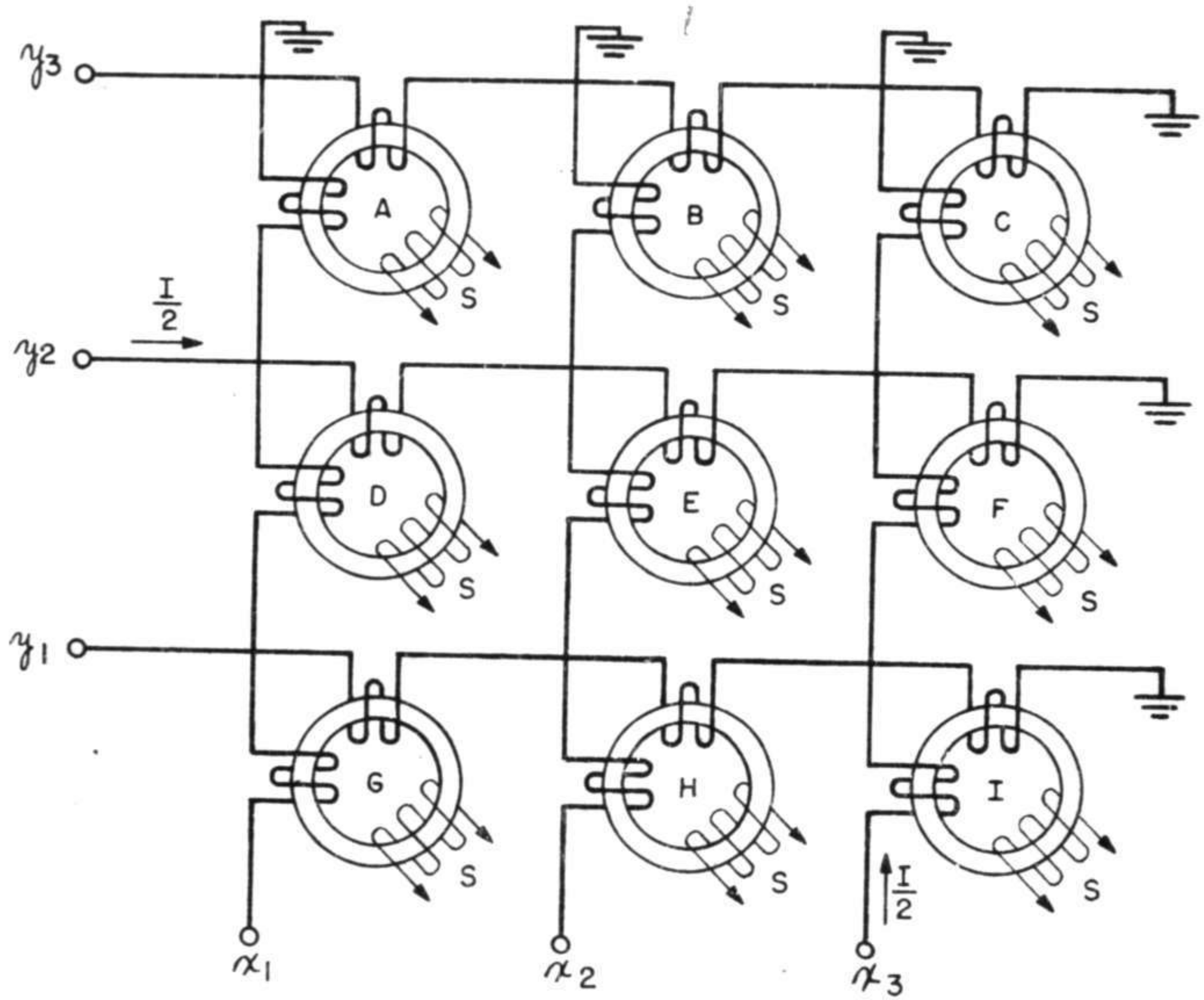

A TWO-DIMENSIONAL ARRAY OF CORES

FIG. 3

The extension to three dimensions may be accomplished by stacking two-dimensional arrays, like the one of Figure 3, in back of each other, with respective x and y lines connected in common. In this arrangement the selection of lines x_ℓ and y_m energizes a vertical plane and a horizontal plane in the array as shown in Figure 4.

This results in the selection of a line $x_\ell y_m$ along which all cores have full magnetizing force impressed. The rest of the cores in the x_ℓ and y_m planes have only half-magnetizing force impressed; cores out of those planes have none.

All that is necessary now is to have a third set of magnetizing (selecting) windings on the cores, connected together in each z plane, and so wound, for each core, as to result in a magnetizing force equal to $-H_M/2$ for an applied current of $-I_M/2$. The application of $-H_M/2$ to each z plane except, say, z_n, will result in magnetizing forces of only $H_M/2$ left on each core in the line $x_\ell y_m$, except for the core at the junction of this line and the z_n plane, core $x_\ell y_m z_n$, which is the selected core.

For the Whirlwind I computer, the z planes might well represent the 16 digits of the number on the number bus, while two 32-position switches control the x and y coordinates for selecting the desired register (or word) from the 1024-register storage array.

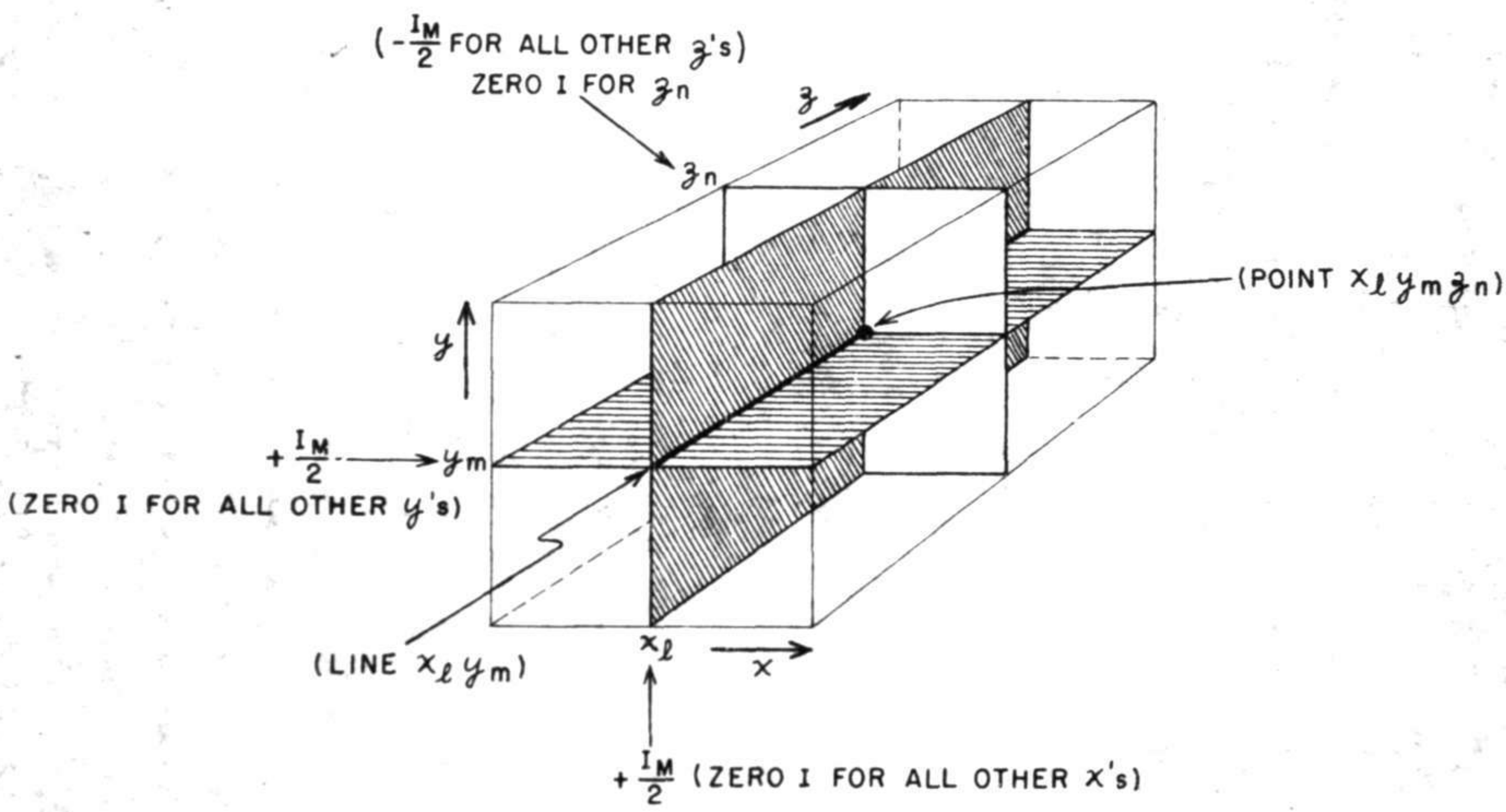

A THREE-DIMENSIONAL SELECTION SCHEME

FIG. 4

D. Attack on the Problem

At the start, and during some of the earlier stages of the work, it became apparent that two courses of attack on the problem were possible. One involved doing a great deal of detailed, rigorous research of a theoretical nature, and amassing experimental data on some very limited portion of the problem. The other involved keeping analysis and data-taking at a minimum, and consisted of a quick development program designed to demonstrate the practicability of the concept and to give a survey of available materials.

The decision made leaned, in general, in the latter direction. It was felt that a greater contribution to the art was to be made by obtaining an early, though rough, assessment of the potentialities of magnetic cores for use in this three-dimensional storage scheme. Accordingly, the development of core-testing equipment to fill these needs was pushed hard, as was the obtaining and processing of sample cores. Some time had to be spent on analysis of the eddy-current shielding problem in order to proceed intelligently with the development work, and this was done.

The development work culminated in the test operation of two different cores which bracket the response-time and information-retention parts of the problem very well. The results give a rather dramatic demonstration of the feasibility of the three-dimensional magnetic-storage scheme, at least insofar as the individual units are concerned, and are considered to justify the course taken.

CHAPTER II

CORE RESPONSE TIMES

A. Factors Governing Response Times of Magnetic Materials

The magnetic state of a sample of ferromagnetic material is a function of time as measured from the start of some excitation. Factors entering into the function include losses, aging and like phenomena, and eddy-current shielding.

Losses in the material, as well as in the driving circuitry, affect the shape of a plot of applied magnetizing force (H_e) versus time. A discussion of the response of a magnetic core as indicated by magnetizing force (H) or flux density (B) at points in the material may postulate a given H_e function and, consequently, may sidestep the question of losses. This is done here. H_e is applied as a "rectangular" pulse with a rise time less than 1/2 microsecond; for most of the materials tested this may be considered a step function.

Long- and short-term aging phenomena, "residual losses",[4] and dimensional resonances[5] are ignored. It is assumed that these are not first order effects during the time intervals used, and that the magnetic moment at a point in a material responds immediately to a change in H at that point.[6] Experimental results indicate that these are reasonable assumptions for a first approximation to the behavior of the cores tested.

B. Eddy-Current Shielding in Thin Tape

When eddy-current shielding is the only significant factor in the response time of a magnetic material, the formulas governing H and B at points in the material, for a step-function of externally applied H, may be derived from Maxwell's Equations. (See Appendix.) If displacement currents may be disregarded and "semi-infinite-plate" geometry is assumed for the material (both of which may be done for a thin metallic tape or ribbon) one resultant set of formulas is:

$$\frac{\partial^2 H}{\partial x^2} - \sigma \frac{\partial B}{\partial t} = 0, \quad \text{where } \sigma \text{ is the conductivity of the material;} \tag{4}$$

$$B = f(H). \tag{5}$$

When B is a multi-valued and non-linear function of H, the problem of solving the equations is beyond present-day techniques. If the multi-valuedness of the functions may be disregarded (as in the case where half of one particular loop in the B-H plane is being travelled) the solution is more easily accomplished. The single-valued linear case is discussed first, followed by the single-valued non-linear case.

Theoretical discussion is confined to the thin-tape shape because all of the presently useable metallic cores are wound of thin tape, the ferritic cores which have square or rectangular cross sections have extremely high resistivities and rather low permeabilities so that eddy currents are almost negligible in them.

and finally, the qualitative concepts, which derive easily for thin tape, hold in a general way for all shapes.

1. <u>The Linear Case</u>

When f(H), above, is not only single-valued but also linear, we may define a constant, called the permeability, $\mu \equiv B/H$, and the solution for H becomes (see Appendix for derivation):

$$\frac{H}{H_e} = 1 - \frac{4}{\pi} \sum_{n=1}^{\infty} \frac{1}{n} \sin \frac{n\pi}{a} x \; e^{-n^2 \frac{t}{\tau}}, \qquad \text{for odd } n, \tag{6}$$

$$\tau \equiv \frac{a^2 \sigma \mu}{\pi^2}. \tag{7}$$

Where: a is the thickness of the ribbon, or tape; x is measured from the surface of the tape into the material; H_e is the magnitude of the applied step-function of H; <u>the material was unmagnetized at the start</u>.

Figure 5 shows H/H_e plotted versus t/τ for four values of x. It is interesting to note that the curves leave the origin with zero slope, with the trivial exception of the curve for x = 0.

In Figure 6, H/H_e is plotted versus x for various values of t/τ. Since we assume that the flux density, B, is linearly proportional to H, these curves show the growth of B/B_e as a function of time throughout the material. The flux, ϕ, is proportional to

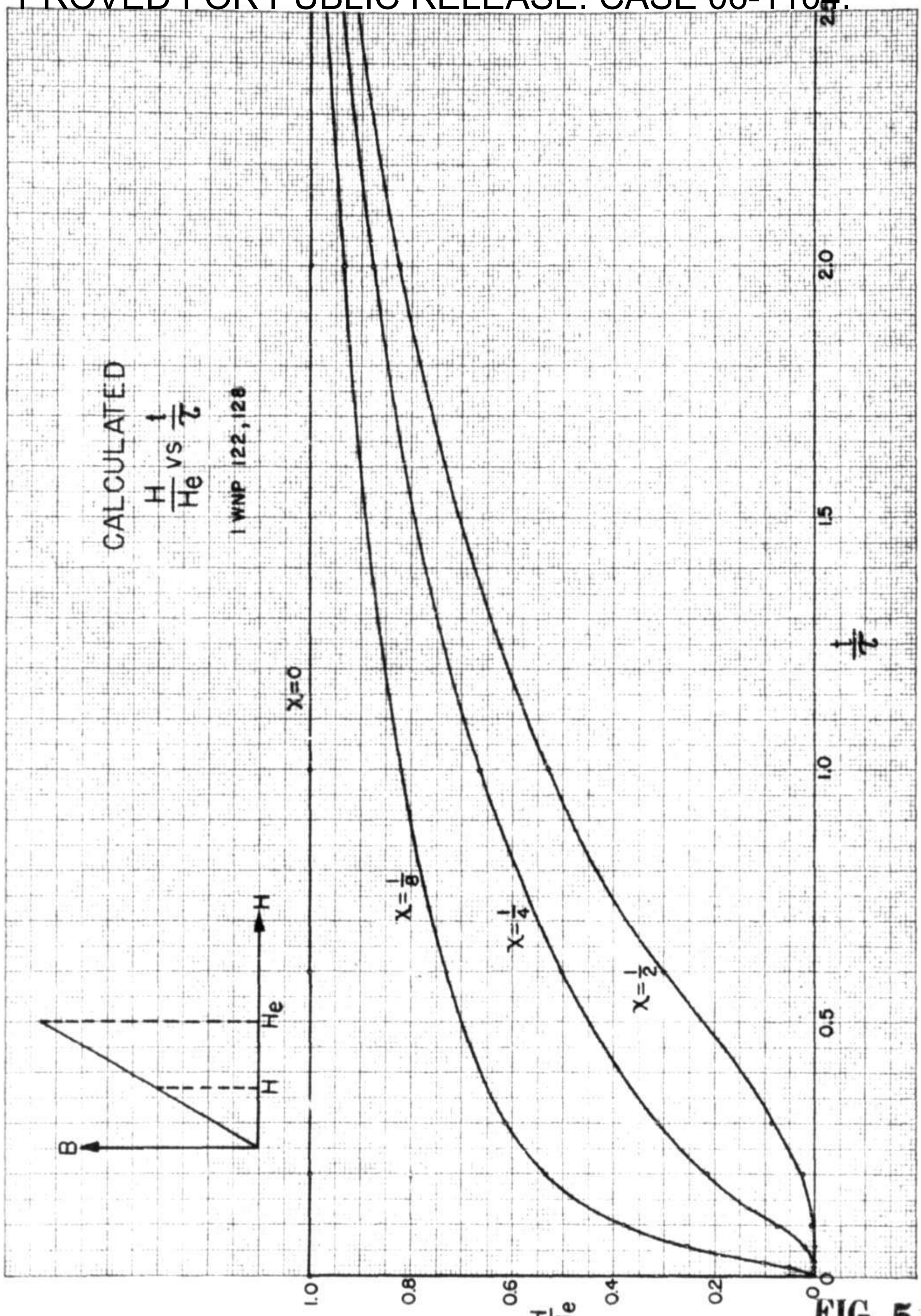
CALCULATED
H/He vs t/τ
I WNP 122, 128
X=0
X=1/8
X=1/4
X=1/2
B
H
He
H/He
t/τ
1.0
0.8
0.6
0.4
0.2
0
0.5
1.0
1.5
2.0
2.5

FIG. 5

A-48009

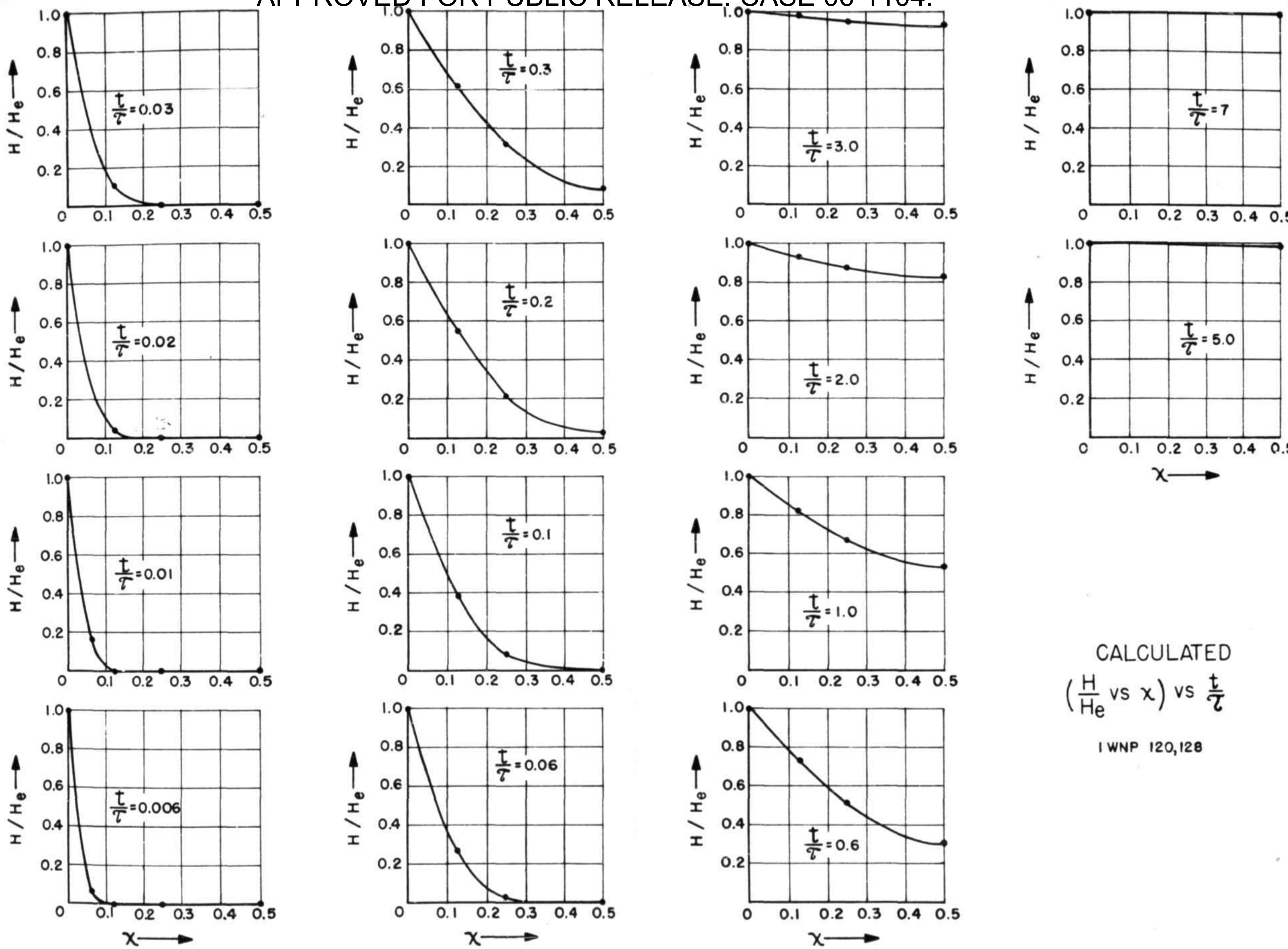

CALCULATED

$\left(\frac{H}{H_e} \text{ vs } \chi\right) \text{ vs } \frac{t}{\tau}$

1 WNP 120,128

FIG. 6

$\int B\,dx$, or the area under each curve. A plot of these areas versus t/τ is shown in Figure 7a; this plot may also be arrived at by properly weighting and summing the curves in Figure 5. Note that near the origin the effects of the outside portions of the material (small x values) predominate, and the curve reaches its maximum slope for extremely small values of t/τ so that, for all practical purposes, it may be assumed to leave the origin with maximum (but finite) slope. The slope is plotted in Figure 7b; it is linearly proportional to $d\phi/dt$, so that it shows the shape of the voltage pulse, e_s, which appears across a sensing coil wound on the core. The pulse has its maximum amplitude at, or very near, the origin and falls off from there on out. The pulse amplitude is negligible by the time $t = 7\tau$.

2. <u>The Non-Linear Case</u>

When the function f(H), eq. (2), is single-valued but not linear, equations (4) and (5) combine to give:

$$\frac{\partial^2 H}{\partial x^2} - \sigma \frac{\partial f(H)}{\partial t} = 0. \tag{8}$$

The function f(H) is commonly described by drawing the pertinent portion of the pertinent hysteresis loop for the material. Such a curve is shown in Figure 8 for one of the more satisfactory experimental cores. It is obviously highly non-linear and not easily described by any simple analytical expression. This is unfortunate, for equation (8) becomes separable when f(H) is a reasonably simple power of H, such as $H^{1/3}$.

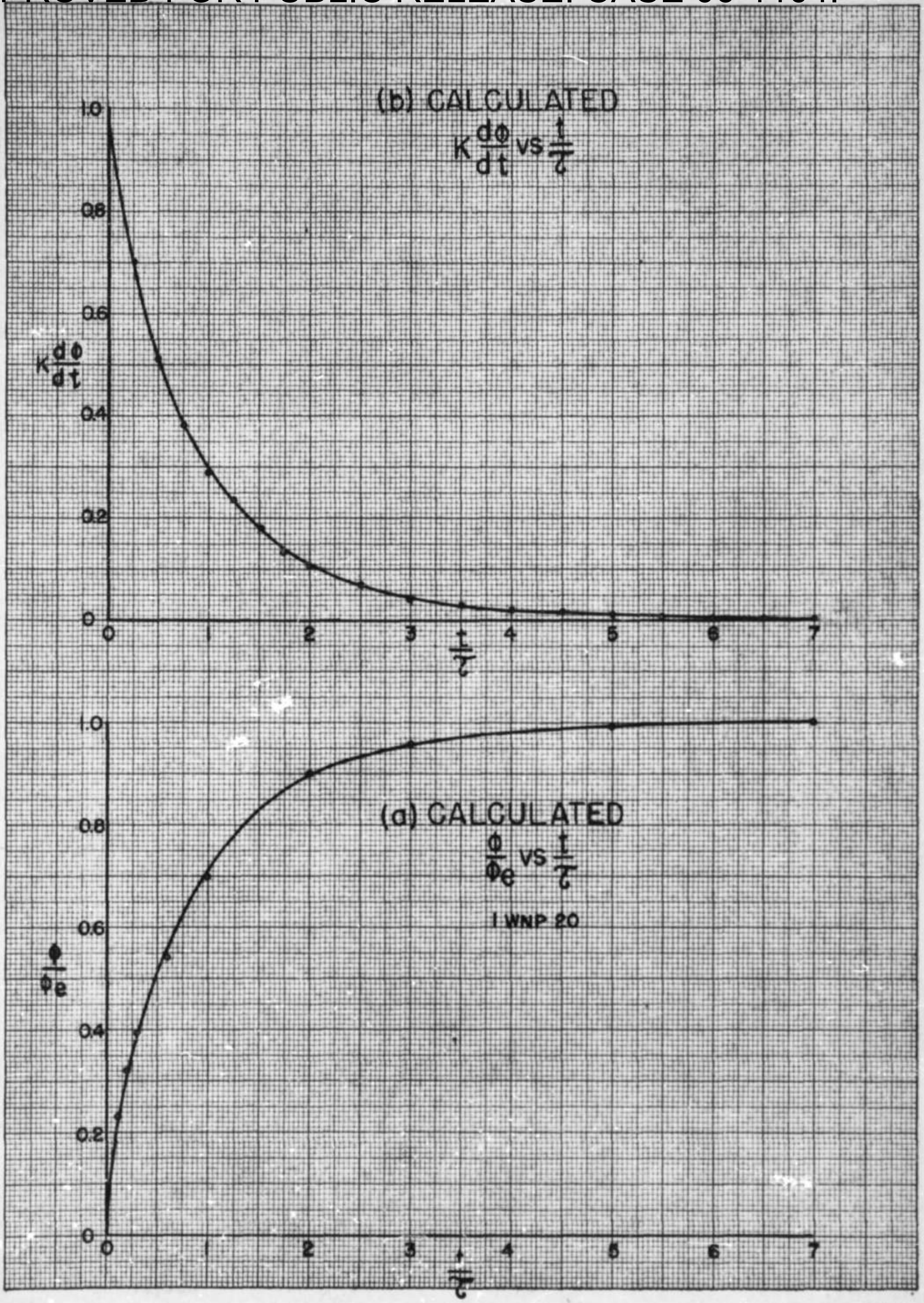
(b) CALCULATED
K dϕ/dt vs t/τ
1.0
0.8
0.6
K dϕ/dt
0.4
0.2
0
0
1
2
3
t/τ
4
5
6
7
1.0
(a) CALCULATED
ϕ/ϕe vs t/τ
1 WNP 20
0.8
0.6
ϕ/ϕe
0.4
0.2
0
0
1
2
3
t/τ
4
5
6
7

A-48002

FIG. 7

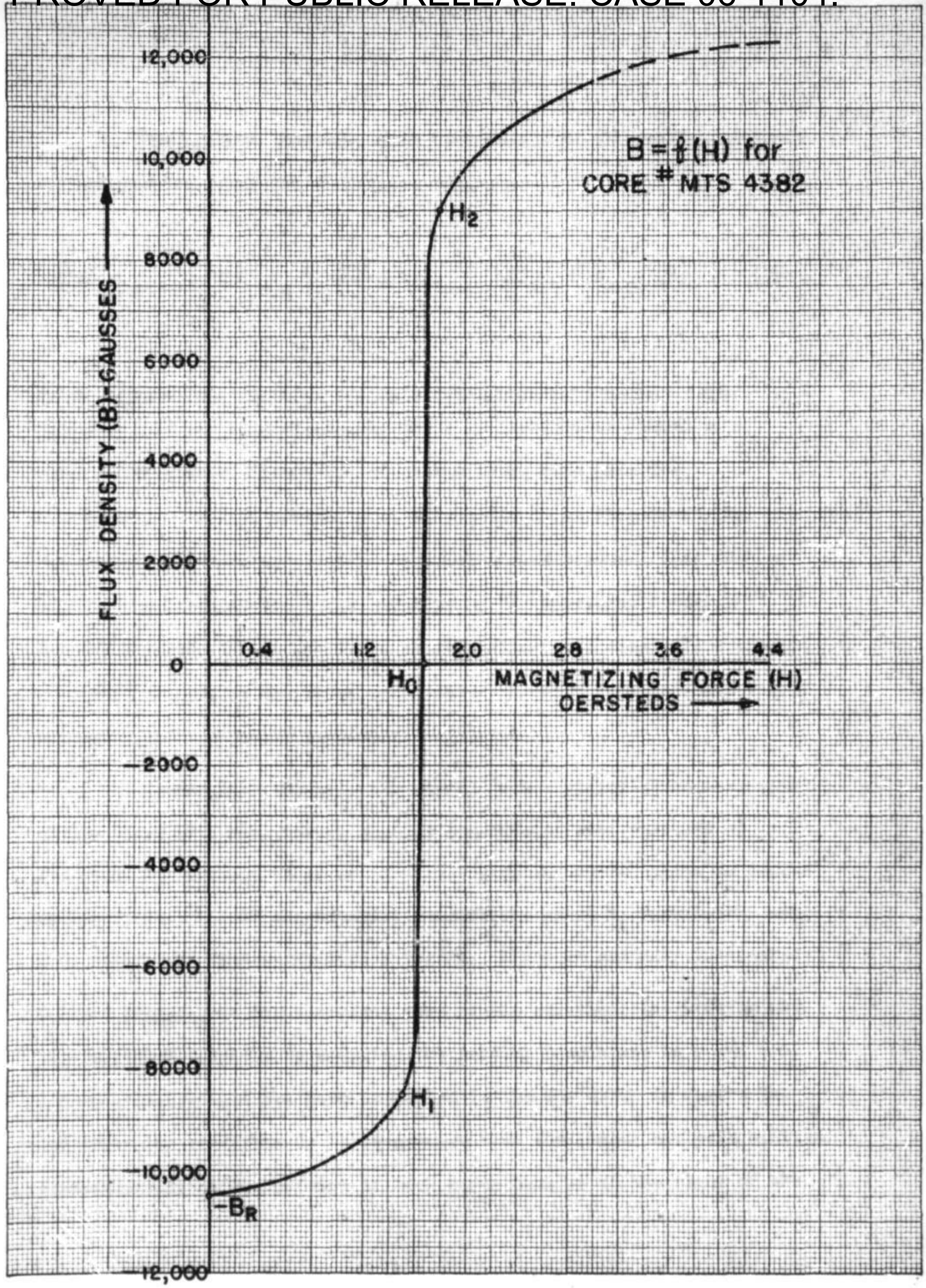
12,000
10,000
8000
6000
4000
2000
0
-2000
-4000
-6000
-8000
-10,000
-12,000
FLUX DENSITY (B)-GAUSSES
0.4
1.2
2.0
2.8
3.6
4.4
MAGNETIZING FORCE (H)
OERSTEDS
$B = f(H)$ for
CORE # MTS 4382
H_2
H_0
H_1
$-B_R$

FIG. 8

A-48003

The problem, however, does lend itself to a numerical analysis. One was started using the difference equation.

$$f(H)_{x,\ t+\Delta t} = f(H)_{x,t} + \frac{\Delta t}{\sigma(\Delta x)^2}\left(H_{x+\Delta x,t} - 2H_{x,t} + H_{x-\Delta x,t}\right), \qquad (9)$$

which follows from equation (4) in a straightforward manner. The function f(H) was approximated by three straight lines fitted to a curve like that of Figure 8, and calculations made on a desk calculator. The work proved to be very tedious and time-consuming, and was abandoned before any conclusive results were reached. The problem will be prepared, instead, for solution by the Whirlwind I computer, and the results will be available shortly after this thesis is written. The need for a quick and rough qualitative solution remained, and the following approximations suggested themselves.

Assume that the material starts from a steady-state condition at the point $-B_R$, and, for an applied magnetizing step function of amplitude H_e, follows along an idealized path in the B-H plane as drawn in Figure 9a. All of the material reaches the point H_1 immediately and then enters the high-permeability region. Since we are only interested in flux changes, or the transient part of the solution, the problem may be simplified slightly by changing the initial conditions to $H = B = 0$, and considering that the path travelled is the one drawn in Figure 9b. Referring now to Figure 6, it is assumed that the linear analysis applies, approximately, to the portion of each curve that is to the right of the

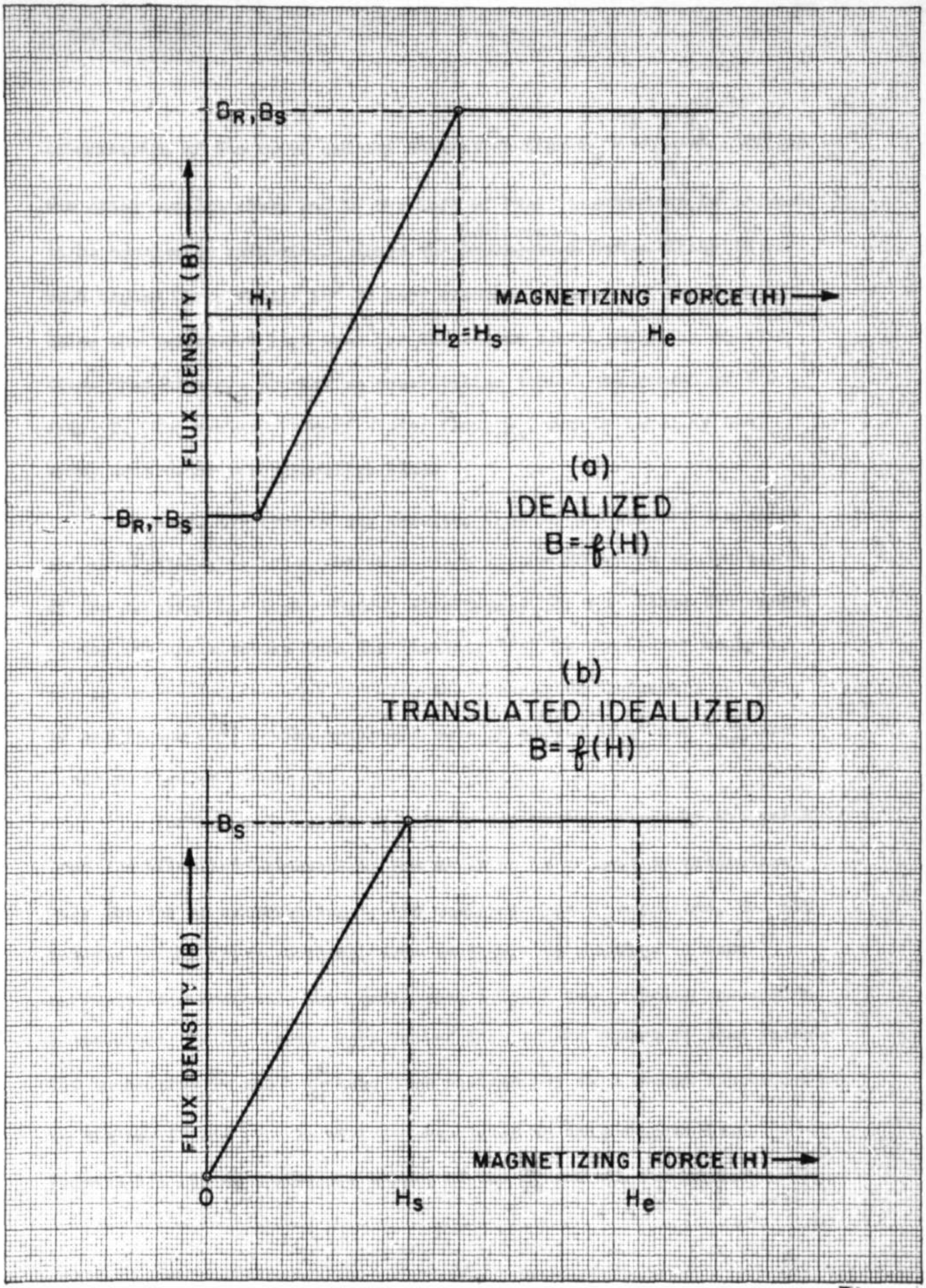

B_R, B_S
FLUX DENSITY (B)
H_1
MAGNETIZING FORCE (H)
H_2=H_S
H_e
-B_R, -B_S
(a)
IDEALIZED
B=f(H)
(b)
TRANSLATED IDEALIZED
B=f(H)
B_S
FLUX DENSITY (B)
MAGNETIZING FORCE (H)
0
H_s
H_e

FIG. 9

A-48032

intersection of the curve and the saturation-line $H_s = \frac{H_2 - H_1}{H_e}$. All of the cross section above and to the left of that intersection is assumed to be completely saturated. Since the ~~incremental~~ differential permeability is very much higher (by a factor 10^5 in many practical cases) for the region below the saturation line than for the region above, only the squares below that line are counted as contributing toward the growth of the flux, ϕ. The maximum (steady state) flux, ϕ_s, may be taken as the total area under the saturation-line.

Also, the lack of any changing flux to the left of the curve and saturation-line intersection means that the effective thickness, a, of the material has been reduced, accordingly, to a_n. Since the square of the thickness enters into the quantity t/τ in the linear analysis, one approximation includes reducing the successive increments of t/τ by the factor $(\frac{a_n}{a})^2$. The resultant sets of curves of $\frac{\phi}{\phi_s}$ and $K \frac{d\phi}{dt}$ are drawn in Figures 10 and 11.

Further speculation on this approximation brings up the point that the effective thickness of the material is reduced by saturation only insofar as contribution to the changing flux is concerned, but not insofar as the cross-sectional area available to the flow of eddy currents is concerned. This would seem to call for reducing successive $\frac{t}{\tau}$ increments by the factor $(\frac{a_n}{a})$ rather than by the square of that ratio. The quantities $\frac{\phi}{\phi_s}$ and $K \frac{d\phi}{dt}$ have been plotted for this second approximation in Figures 12 and 13. As will be seen later in this chapter (see Figures 17, 18, 20A, 20B) the shapes of the $\frac{d\phi}{dt}$ curves, for either

A-48005

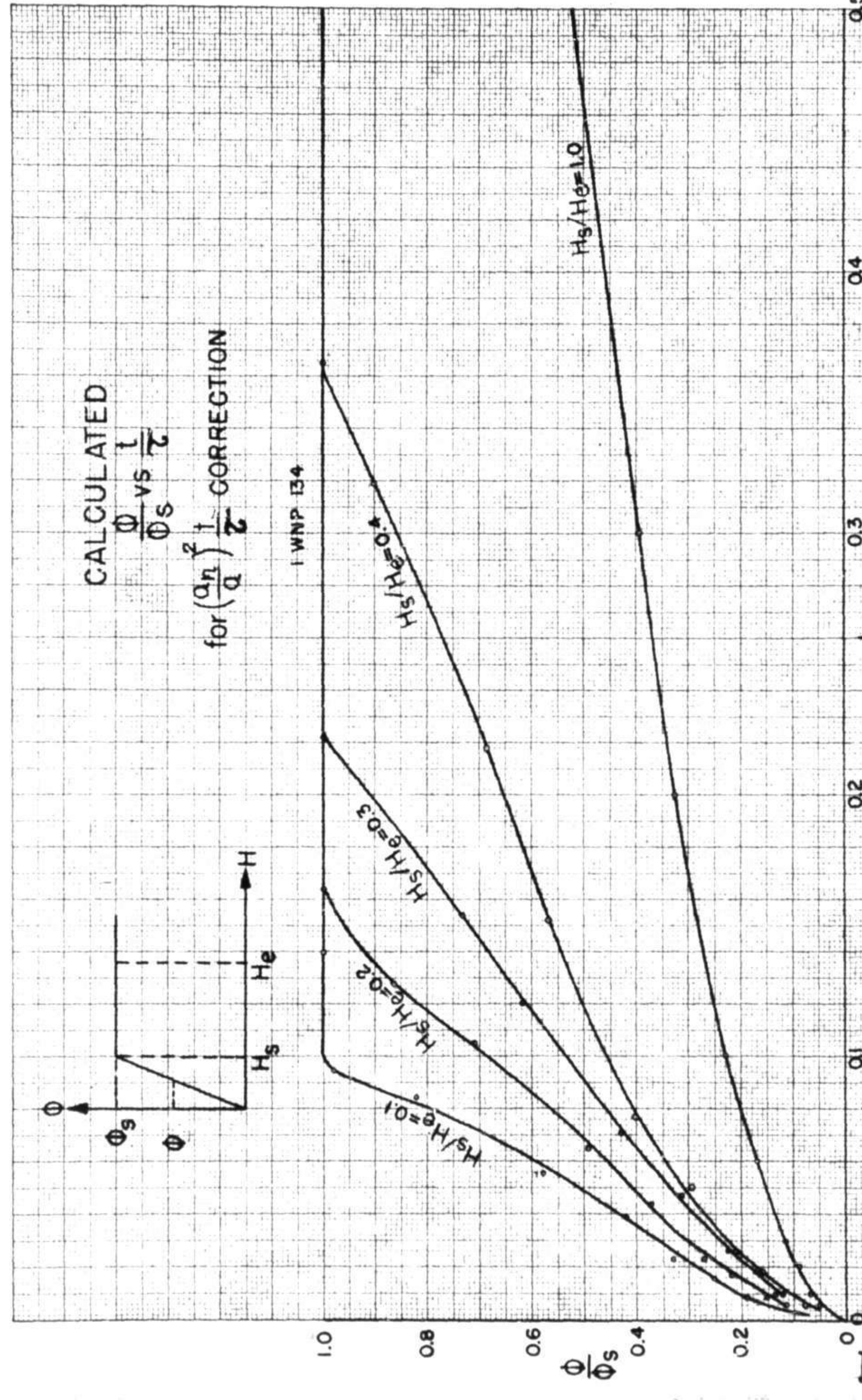

FIG. 10

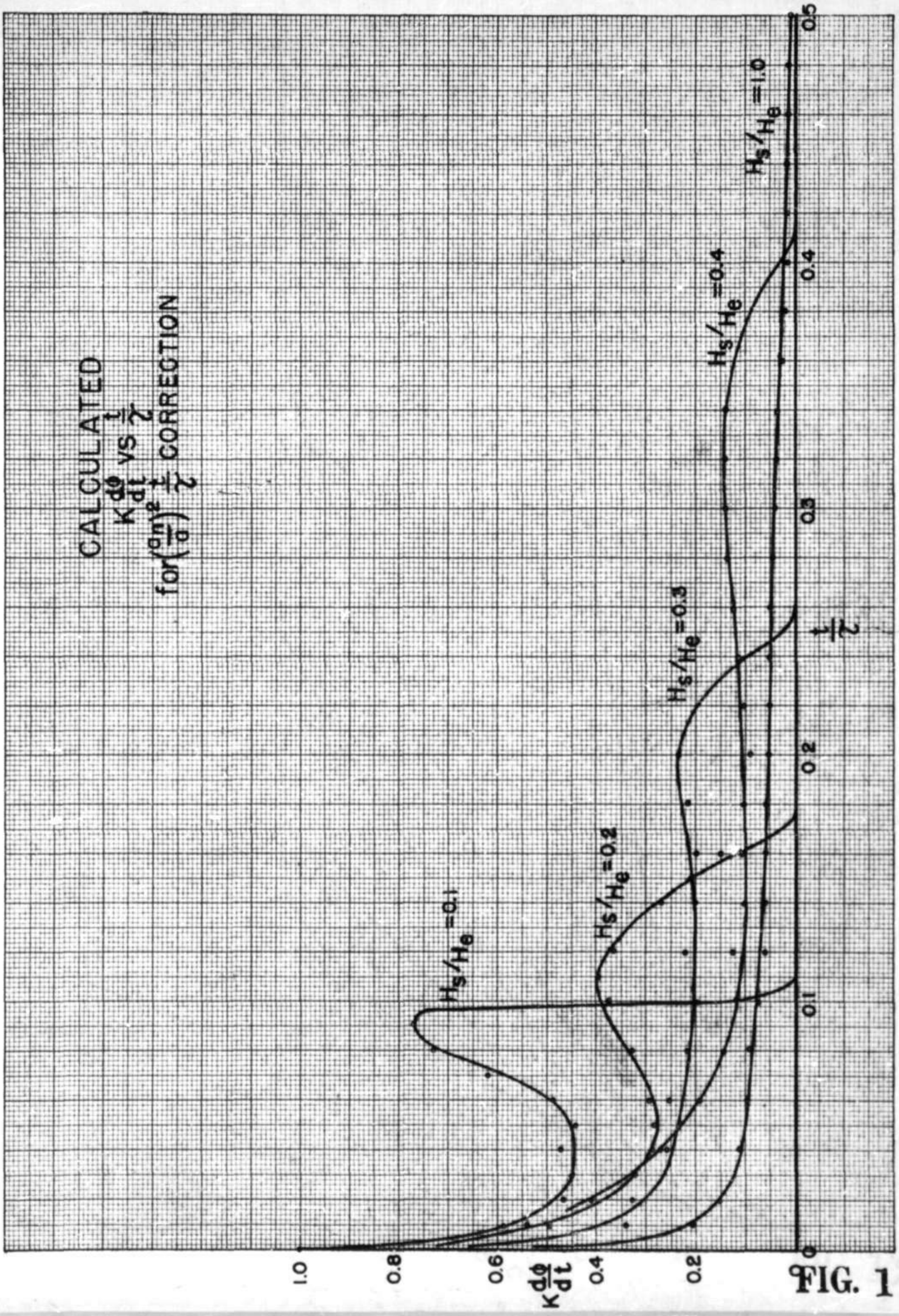

FIG. 11

A-48006-G

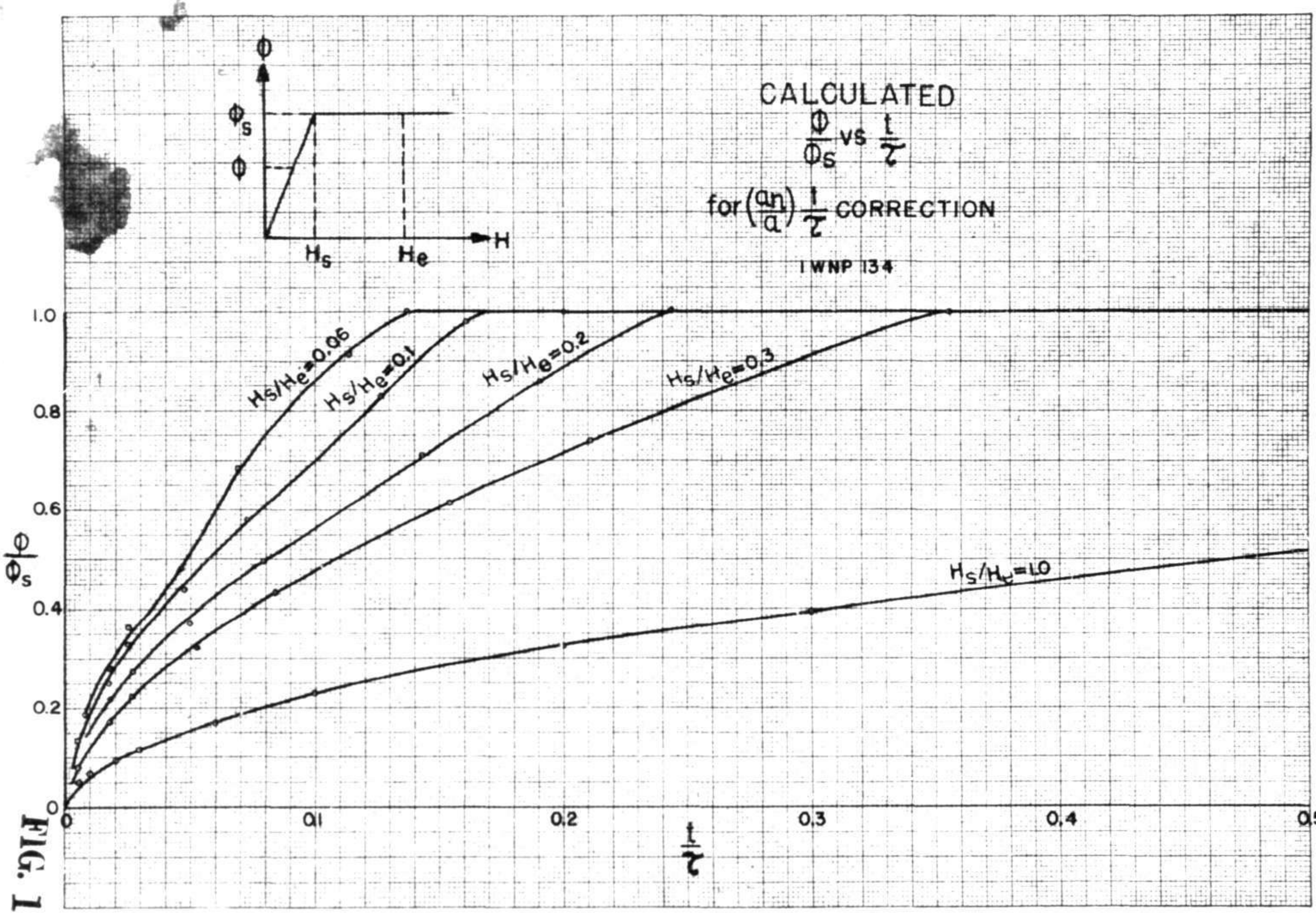
CALCULATED
$\frac{\Phi}{\Phi_S}$ vs $\frac{t}{\tau}$
for $\left(\frac{a_n}{a}\right)\frac{t}{\tau}$ CORRECTION
I WNP 134
Φ
Φ_S
Φ
H_S
H_e
H
$H_S/H_e=0.06$
$H_S/H_e=0.1$
$H_S/H_e=0.2$
$H_S/H_e=0.3$
$H_S/H_e=1.0$
$\frac{\Phi}{\Phi_S}$
0
0.2
0.4
0.6
0.8
1.0
0.1
0.2
0.3
0.4
0.5
$\frac{t}{\tau}$

FIG. 12

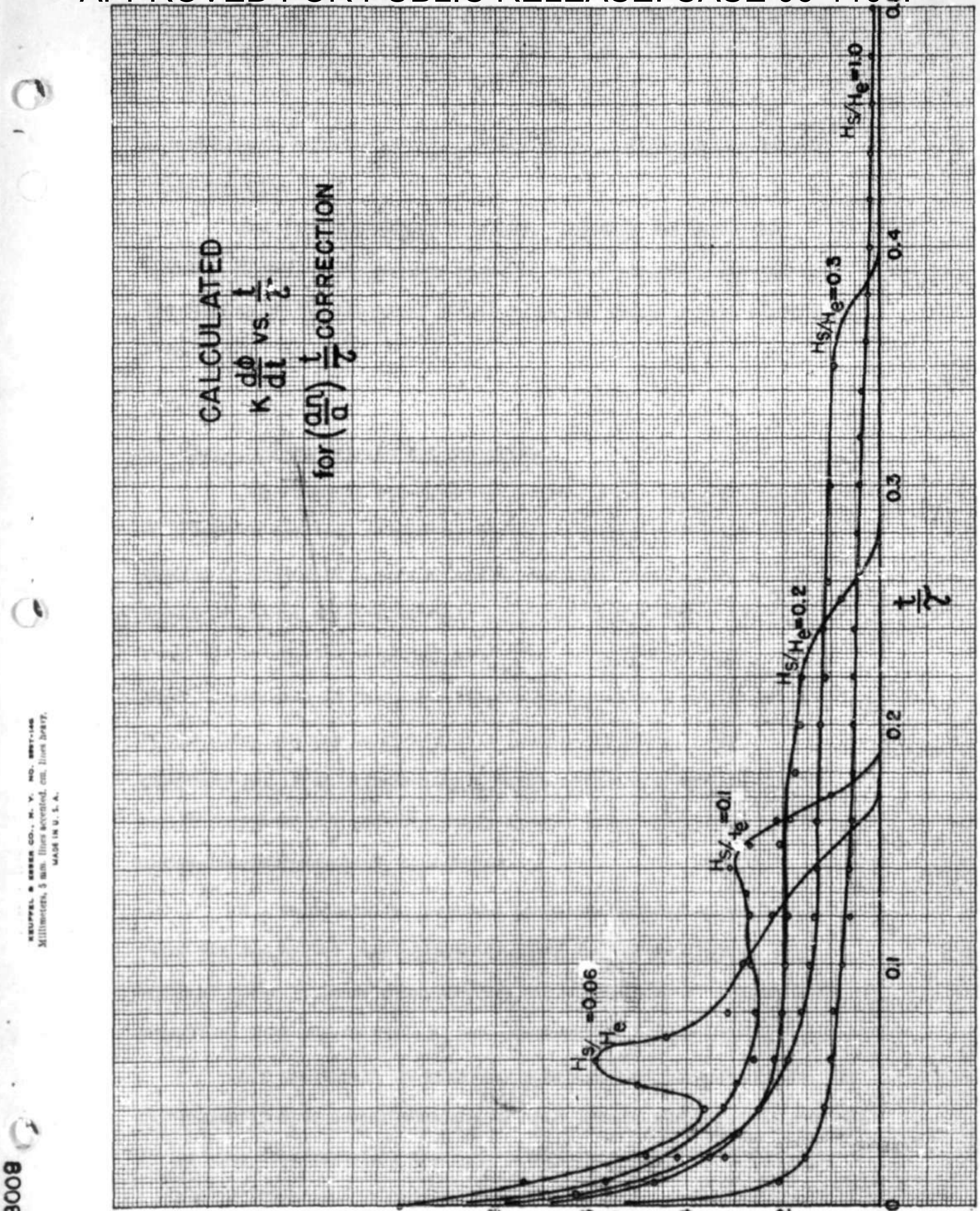
CALCULATED
K dφ/dt vs. t/τ
for (da/a) t/τ CORRECTION
Hs/He = 0.06
Hs/He = 0.1
Hs/He = 0.2
Hs/He = 0.3
Hs/He = 1.0
K dφ/dt
t/τ
0
0.1
0.2
0.3
0.4
0.2
0.4
0.6
0.8
1.0
A-48008

FIG. 13

approximation, bear a fair resemblance to the output pulses obtained experimentally.

Further theoretical judgement regarding the value and validity of the approximations requires deeper analysis, particularly the results of the numerical solutions as the computer will perform them.

C. Experimental Results and Comparisons

Experimental determination of the static magnetic state of a core is not conveniently obtained. A dynamic picture of the changes occurring in a core is easily recorded, however, as a family of curves showing the rate of change of flux, $\frac{d\phi}{dt}$, versus time, t, for applied step functions of H at varying amplitudes, H_e. These curves are, in fact, the voltage pulses induced in a winding on the core, and may be viewed on a cathode ray oscilloscope or synchroscope. From such families, more particular pieces of data may be extracted for plotting other curves; e.g., response times (pulse lengths) versus H_e amplitudes.

H_e, incidentally, is taken to be the applied magnetomotive force divided by the mean circumference of the toroidal core. The ratio of outer to inner diameters was close enough to 1 to warrant the assumption that steady-state H_e was constant throughout each metallic core.

For cores with an extremely wide range of response times, and where quantitative comparisons can be made between different thicknesses of the same core material, the data is often presented in the form of curves of response times (pulse lengths) versus H_e amplitudes. This is true largely of the Deltamax cores. For some of the "faster" metallic cores and the ferritic cores, families of pulse shapes are shown and other data extracted where necessary.

Testing was done almost exclusively on cores which have rectangular hysteresis loops.

1. Slow Metallic Cores

The tape-wound Deltamax cores, as supplied by Allegheny Ludlum Steel Corp. or its subsidiary, Arnold Engineering Corp., are very slow cores, largely because of their phenomenally high maximum ~~incremental~~ differential permeability, μ_{di}. From Figure 14, μ_{di}, which is given by the slope of the saturation hysteresis loop as it crosses the H axis, may be obtained as approximately 1.3×10^6 gausses/oersted. Using eq. (7), for 2-mil thick tape, with a resistivity of about 35×10^{-8} ohm-meters, the calculated value for one "time constant", τ, is 1.2 milliseconds. From Figure 7b, the time to the end of the $\frac{d\phi}{dt}$ pulse for the linear case should be about $7\tau \approx 8.4$ milliseconds.

For the actual saturable material (see Figure 14) the above reasoning indicates that as the amplitude of the applied H_e approaches $H_e \approx 0.075$ oersted, the time, t, to the end of the output pulse should approach 8 milliseconds. The curve drawn for the experimentally taken data (see curve marked 2-mil Deltamax on Figure 15) extrapolates to beyond 100 milliseconds for $H_e = 0.075$ oersted. The correlation here is bad due in part to unavoidable inaccuracies in the data, and the fact that

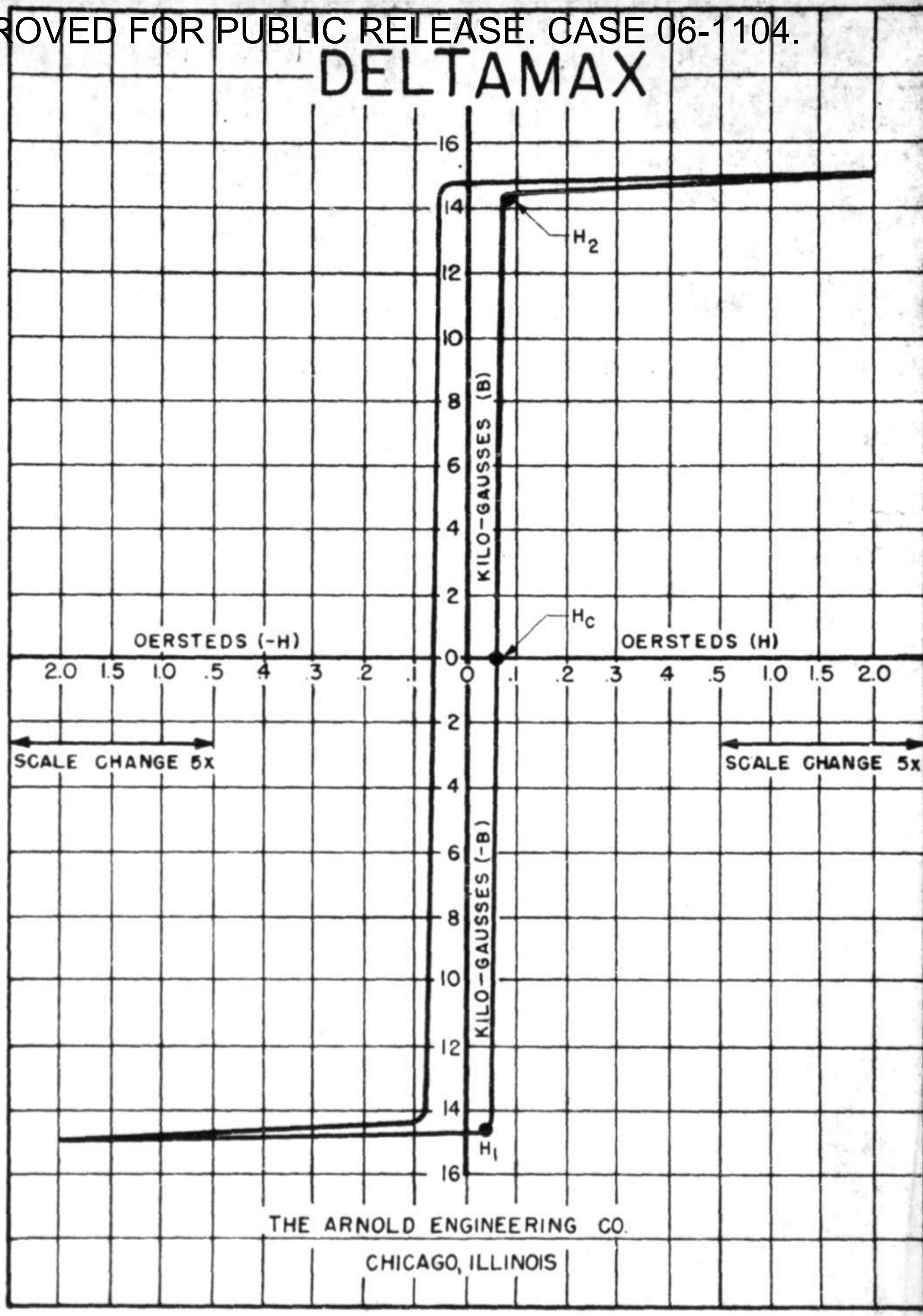

A-48019-

FIG. 14

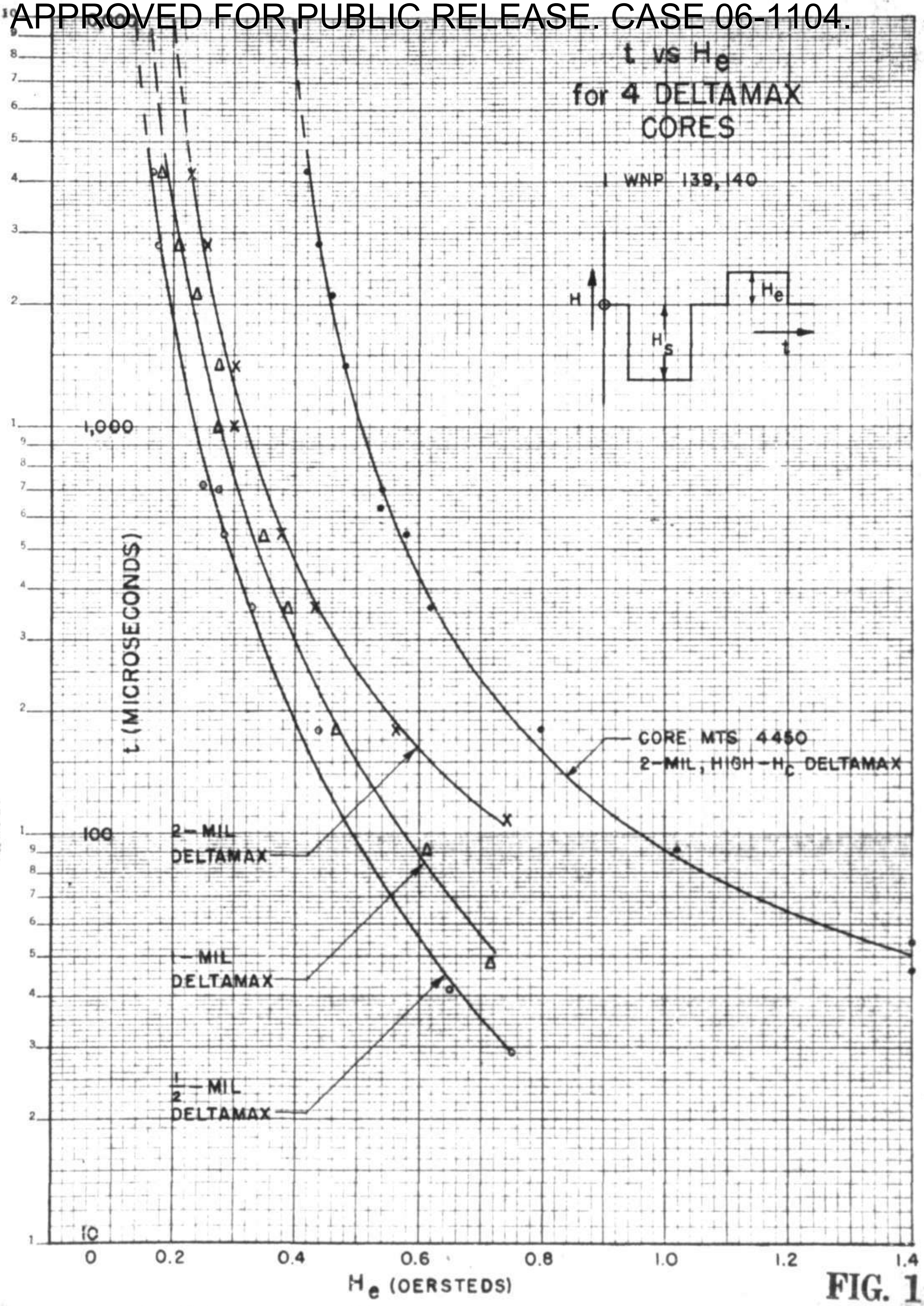

A-48017-G

FIG. 15

interlaminar conduction may not be negligible on these early samples. It is also likely that assumptions mentioned in the third paragraph of this chapter are poorly fulfilled in many cases.

The fourth curve in Figure 15 is for a 2-mil Deltamax core which was processed so as to raise its coercive force, H_c, to about 0.23 oersted. (See Figure 16). It also has a lower maximum differential ~~incremental~~ permeability; $\mu_{di} \approx 0.7 \times 10^6$ gausses/oersted, about half that for regular Deltamax. As $H_e \rightarrow H_2 \approx 0.3$ oersted, the response time of this core should approach about 4 milliseconds; it appears to approach about 100 milliseconds, giving as bad a correlation with linear theory as the other Deltamax cores above.

Correlation with the non-linear approximation of Figures 11 and 13, for $H_s/H_e = H_2/H_e = 0.1$, is fair. The response times of the three cores, expressed as t/τ, where τ is calculated from the physical characteristics of each material using eq. (7), average to 0.18 for the above H_2/H_e ratio. The same pulses from Figures 11 and 13 end at t/τ values of 0.11 and 0.20 respectively. The correlation gets poorer as H_2/H_e gets smaller.

Relative comparisons made between the experimentally taken curves of different cores yield good results. According to the linear theory, τ goes as the square of the tape thickness. For a given H_e, therefore, the three regular Deltamax curves of Figure 15 should be spaced from each other, along the t axis, by a factor of 2^2, or 4.

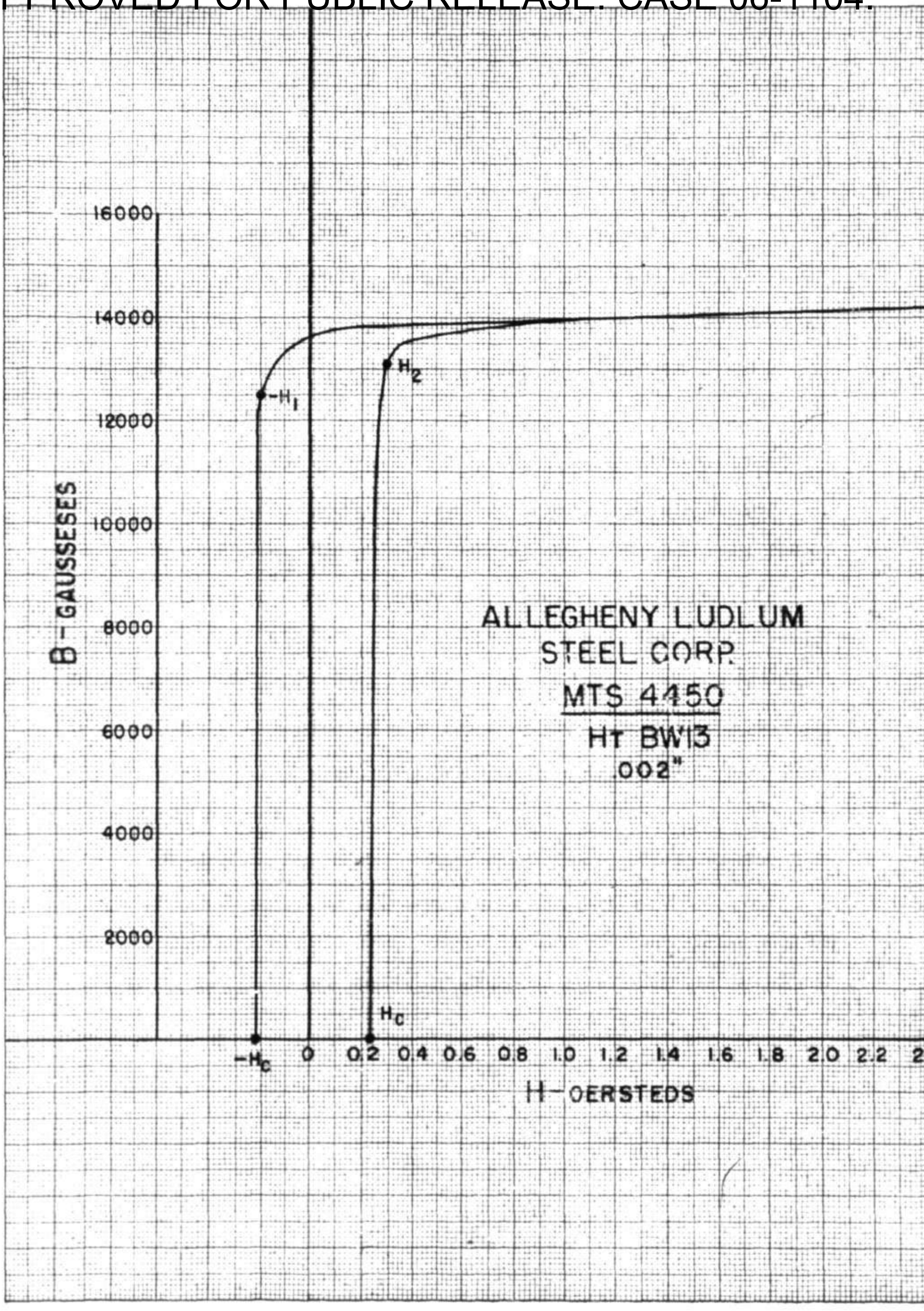
16000
14000
12000
10000
8000
6000
4000
2000
B - GAUSSESES
-H1
H2
Hc
-Hc
0
0.2
0.4
0.6
0.8
1.0
1.2
1.4
1.6
1.8
2.0
2.2
2.4
H - OERSTEDS
ALLEGHENY LUDLUM
STEEL CORP.
MTS 4450
HT BW13
.002"

FIG. 16

This does not hold well for the curves through most of the range shown, but does begin to hold better as the curves come in toward H_2, where the B-H paths approach closer to linearity. For example, at $H_e = 0.2$ oersted, t is about 10 milliseconds for the 2-mil curve and about 3.5 milliseconds for the 1-mil curve. This factor of about 3 decreases to less than 2 for higher H_e values, and appears to increase (possibly to 4) for lower H_e values.

The curve for core MTS 4450 may be compared with the 2-mil curve for Deltamax by comparing response times, t, for small equal increments of H above respective H_2 values. The 2-mil Deltamax, for $H_e = H_2 + 0.125 = 0.2$ oersted has a t of 10 milliseconds; core MTS 4450, for $H_e = H_2 + 0.125 = 0.415$ oersted has a t of about 5 milliseconds. This factor of 2 is very close to the ratio of the μ_{di} values for the two materials. Once again, comparison involving linear theory is good for low H_e values, and poor for high ones where departure from linearity is extreme.

Figures 17 and 18 are photographs of scope traces showing the growth of output pulses as a function of H_e amplitudes for a 2-mil Deltamax core and core MTS 4450. There is some qualitative resemblance between the shapes of the predicted pulses of Figures 11 and 13 and these photographs.

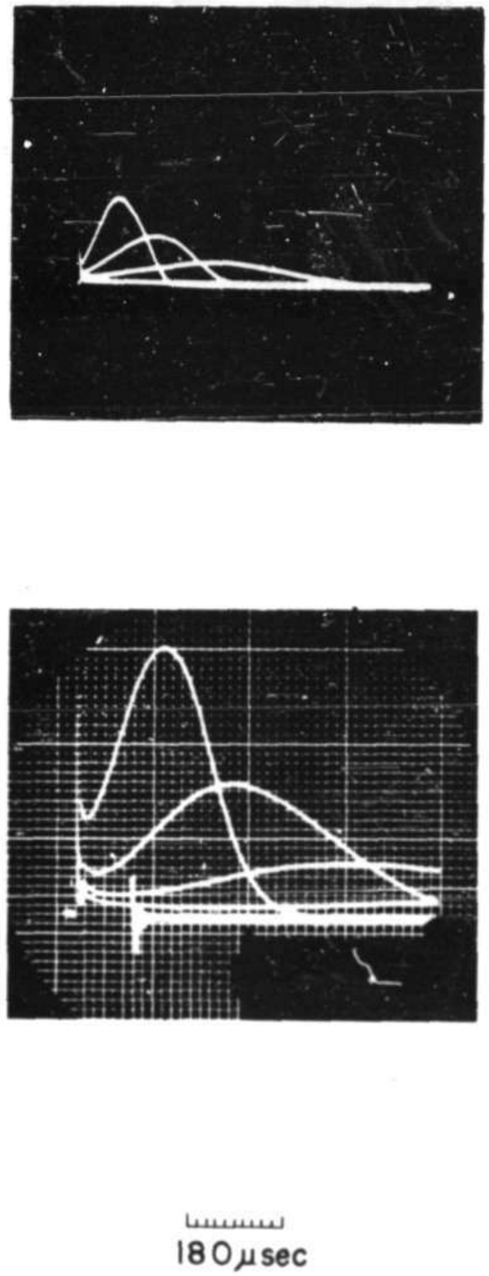

TWO FAMILIES OF OUTPUT PULSES (FOR VARIOUS AMPLITUDES OF APPLIED H_e) FOR A 2-MIL DELTAMAX CORE

FIG. 17

A-35975 F-1111

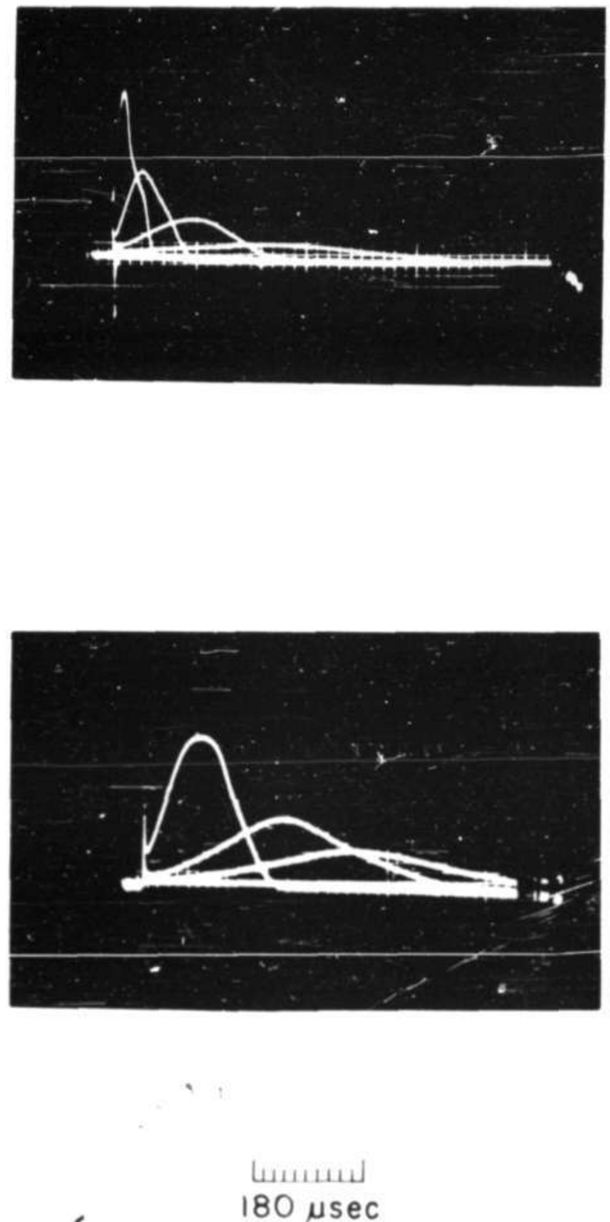

TWO FAMILIES OF OUTPUT PULSES
(FOR VARIOUS AMPLITUDES OF APPLIED
H_e) FOR CORE MTS 4450

A-359-1 · F-1105

FIG. 18

2. Fast Metallic Cores

It is important to recall, at this point, that when a core is used in the coincident-current scheme it is switched by magnetizing forces which are always less than $2H_1$ (see eq. 3, Chapter I). The data in this section extend appreciably beyond $2H_1$, but emphasis is often laid on the region up to that point.

The cores discussed in the previous section are not suitable for use as coincident-current memory units because their response times, for H_a less than $2H_1$, are of the order of milliseconds. If eddy-current shielding, as discussed, is the important time-consuming effect, then the equivalent time constant, τ, of the material is a useful criterion and may be reduced, in a metallic core, by reducing tape thickness, by increasing material resistivity, or by reducing permeability. Unfortunately, it is not practically feasible at present to reduce thicknesses to much below 1-mil or to increase resistivities very much above 50 or 100 microhm-cm in the rectangular-loop metallic materials. Cores are available, however, with substantially lower values of maximum differential ~~incremental~~ permeability. Figure 19 shows a highly-rectangular hysteresis loop, for core MTS 4382, whose maximum differential ~~incremental~~ permeability is about 0.125×10^6 gausses/oersted. This value is lower than that for Deltamax by a factor of about 0.1.

When the coincident-current limitation, $H_{a_{max}} < 2H_1$, is considered it becomes apparent that core MTS 4382 should be faster

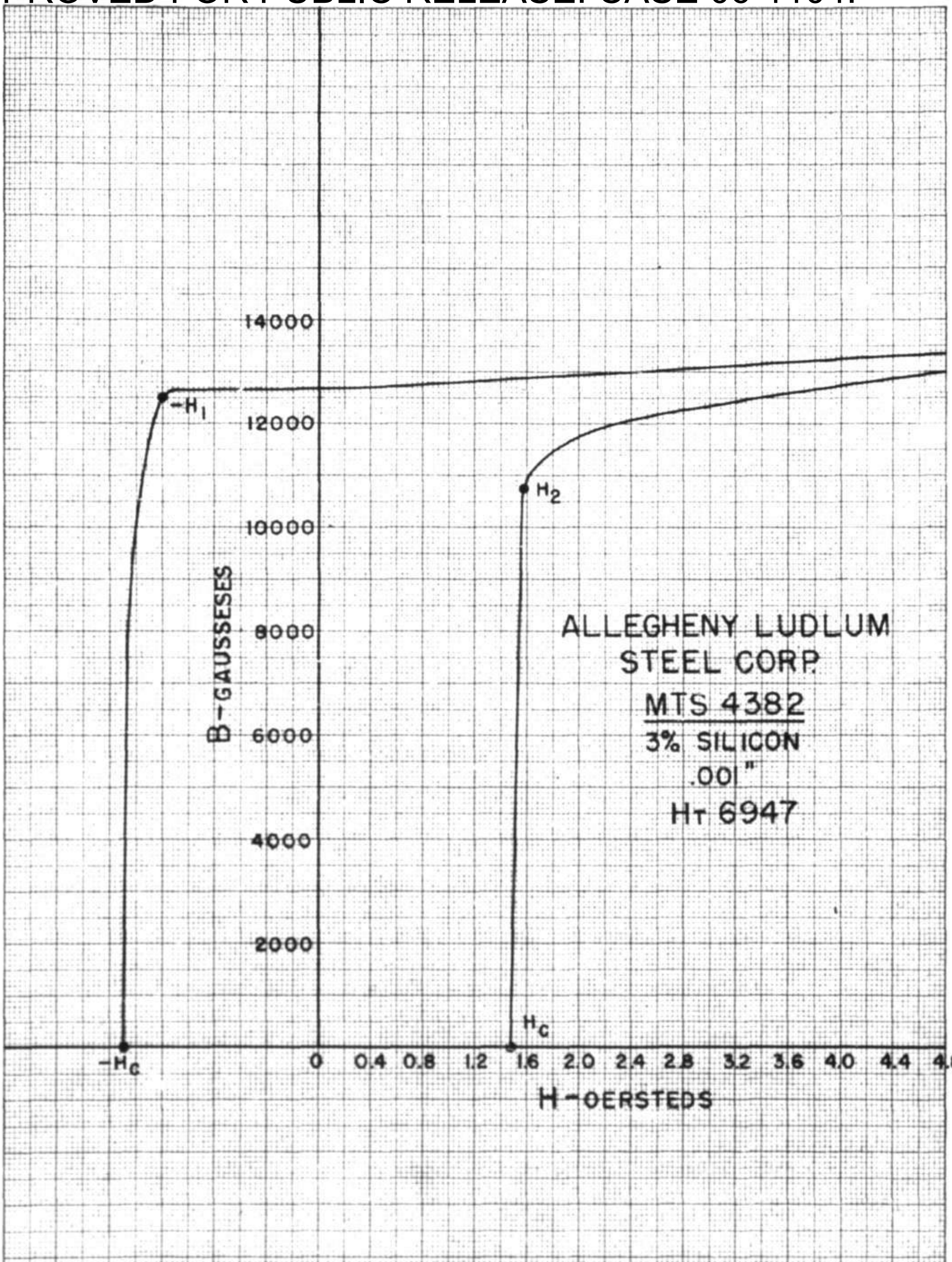

14000
12000
10000
8000
6000
4000
2000
B-GAUSSES
-H1
H2
Hc
-Hc
0
0.4
0.8
1.2
1.6
2.0
2.4
2.8
3.2
3.6
4.0
4.4
4.8
H-OERSTEDS
ALLEGHENY LUDLUM
STEEL CORP.
MTS 4382
3% SILICON
.001"
HT 6947

FIG. 19

than a 1-mil Deltamax core by yet another factor when it is used in the proposed scheme. From the hysteresis loop of Figure 19:

$$H_{e_{max}} \lessapprox 2H_1 \approx 2.3 \text{ oersteds,}$$

$$H_s \approx H_2 \approx 1.6 \text{ oersteds, and}$$

$$H_s/H_{e_{max}} \approx 1.6/2.3 \approx 0.5.$$

Whereas, for Deltamax:

$$H_s/H_{e_{max}} \approx 0.075/0.08 \approx 0.94.$$

A glance at the theoretical approximations to the growth of flux with time for various values of H_s/H_e (Figures 10-13) indicates that steady state is reached much sooner at lower values of H_s/H_e. A very rough extrapolation on Figure 10 indicates that steady state is reached at $t/\tau \approx 0.6$ for $H_s/H_e = 0.5$, whereas for $H_s/H_e = 0.94$ steady state is probably not reached until $t/\tau > 5$.

We would expect, therefore, that core MTS 4382 would be about ten times as fast as 1-mil Deltamax under linear conditions, and perhaps one hundred times as fast when used under non-linear conditions for H_e values in the vicinity of $2H_1$ per respective core. From the experimental 1-mil curve of Figure 15, the response time for $H_e = 0.08$ oersted is of the order of tens of milliseconds. From Figure 20, for $H_e = 2.3$ oersteds, the experimental response time for core MTS 4382 is about 0.7 milliseconds. The factor is of the order of a hundred, as expected.

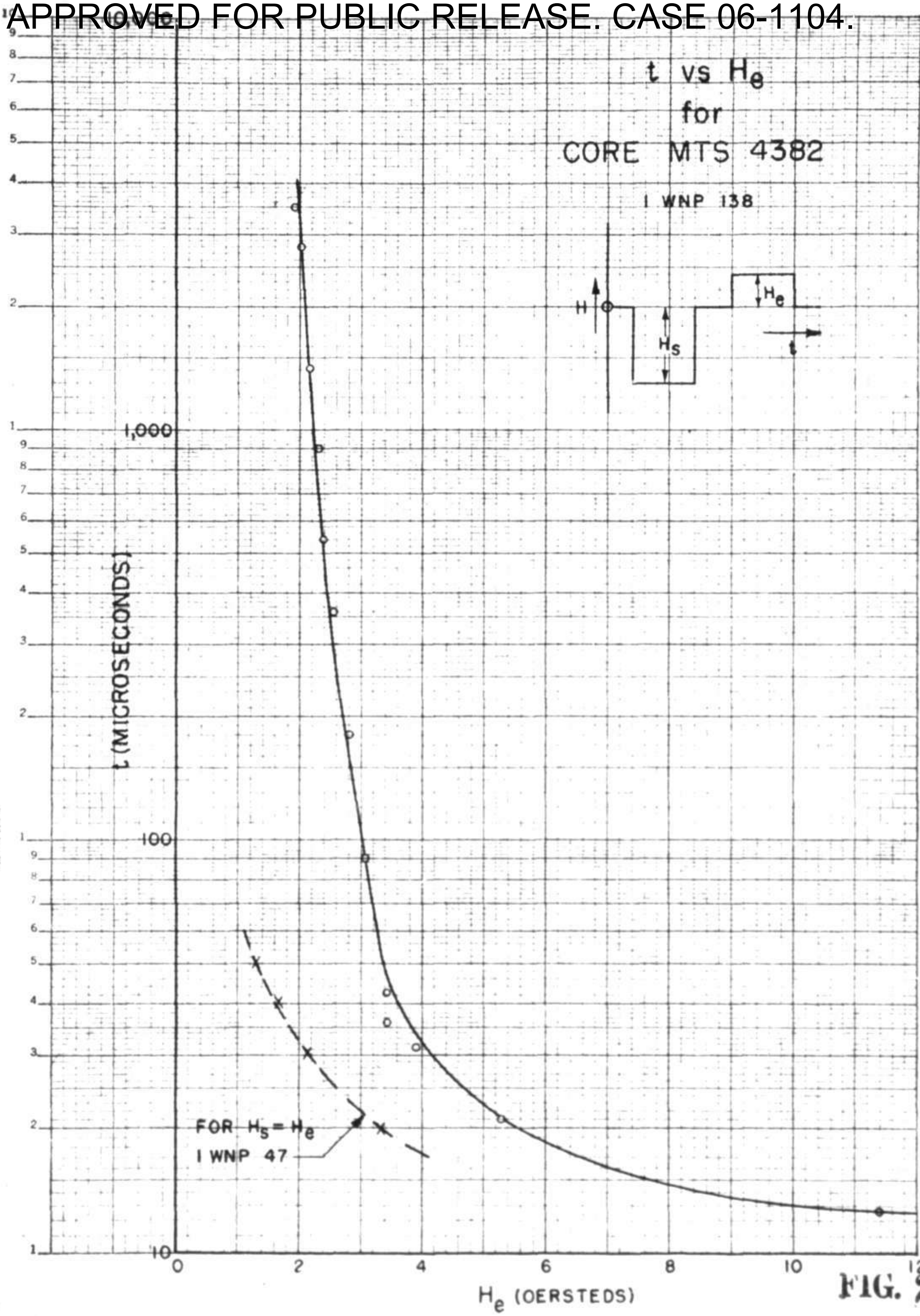

A-48018-G

FIG. 20

Figure 21 shows photographs of a family of output pulses for this core. There is good resemblance in general shape to the curves of Figures 11 and 13.

All of the previous calculations and comparisons have been based on the assumption that a material travelled along its so-called <u>saturation</u> hysteresis loop and that, therefore, the function, $f(H)$, was single-valued, and values of μ_{di} could be taken from those loops as shown in Figure 14, 16, and 19. Because of the need to maintain single-valuedness when attempting to obtain response-time correlations between theory and experiment, most of the data was taken for a material travelling along its saturation loop. This was done by applying asymmetrical magnetizing forces as shown on the small sketches on Figures 15 and 20, where H_s was kept constant at a value sufficient to saturate the core.

Actually, cores will not be worked on saturation loops in the proposed scheme, and it is important to see how response times change when symmetrical excitation is applied and varied. Data taken under these conditions for core MTS 4382 are plotted as the dashed line in Figure 20, and are photographically illustrated in Figure 22. The reduction in response times is very large. The same type of data was taken for Deltamax cores, and is plotted separately in Figure 23. Response times are lowered again, but not as drastically.

As is indicated by additional evidence in the next chapter, the reduction is due largely to the reduction in μ_{di} as inner loops are travelled in the B-H plane. There is also some reduction in

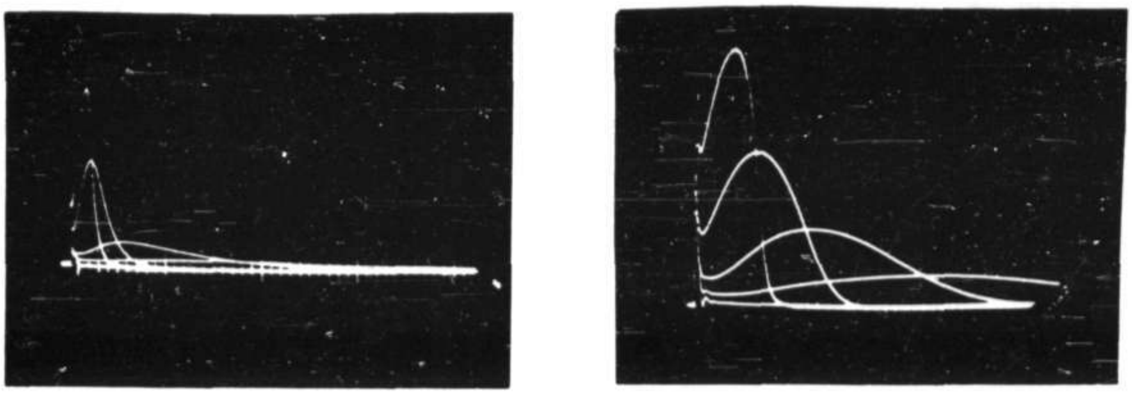

(a) 180 μsec (b) 20 μsec

FIG. 21

TWO FAMILIES OF OUTPUT PULSES (FOR FIVE H_e AMPLITUDES) FOR CORE MTS 4382 UNDER ASYMMETRICAL EXCITATION. NOTE RESEMBLANCE BETWEEN (b) AND THEORETICAL APPROXIMATION TO $d\phi/dt$ IN FIGURE 11.

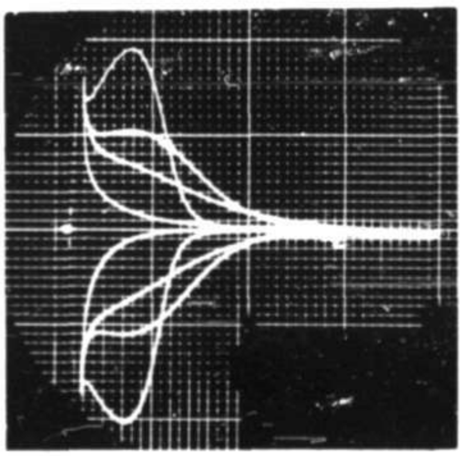

20 μsec

A FAMILY OF OUTPUT PULSES (FOR FOUR H_e AMPLITUDES) FOR CORE MTS 4382 UNDER SYMMETRICAL EXCITATION. NOTE LARGE REDUCTION IN RESPONSE TIMES COMPARED WITH ABOVE.

FIG. 22

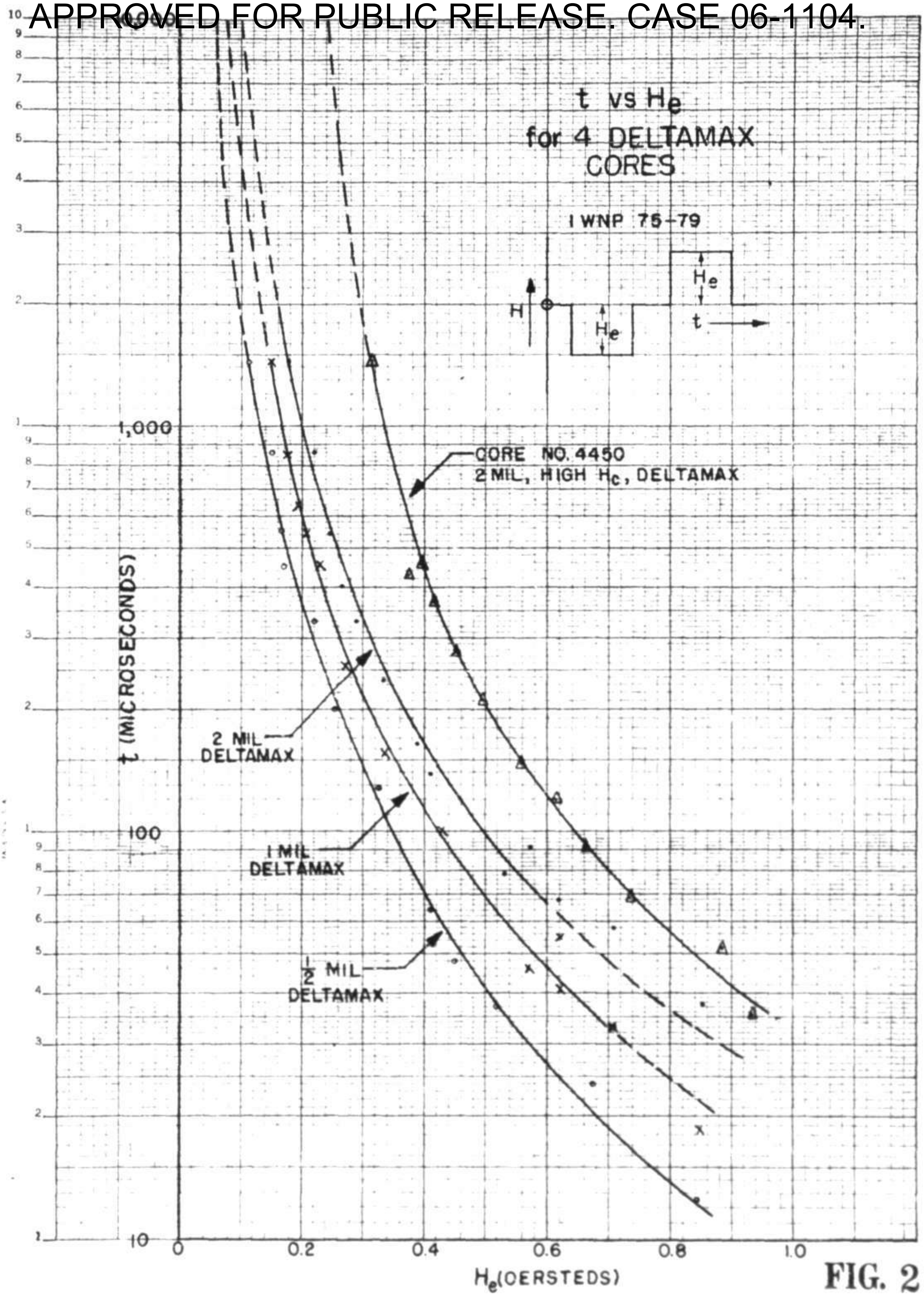

t vs H_e
for 4 DELTAMAX CORES
I WNP 75-79
H
H_e
t
CORE NO. 4450
2 MIL, HIGH H_c, DELTAMAX
2 MIL DELTAMAX
1 MIL DELTAMAX
$\frac{1}{2}$ MIL DELTAMAX
t (MICROSECONDS)
1,000
100
10
0
0.2
0.4
0.6
0.8
1.0
H_e(OERSTEDS)

FIG. 23

retained flux density and in coercive-force values, which would also act to reduce response times for fixed H_s values.

Relative correlations of the above type exist between the already-mentioned metallic cores and others tested. Two which fall under this section's classification are MTS 6464 and MTS 4370, both prepared by Allegheny Ludlum Steel Corp.

3. __Ferritic Cores__

Cores made of the magnetic ferrites promise a major reduction in response times, mainly due to their high resistivities, and secondarily due to their low permeabilities, low saturation flux densities, and high coercivities.

The following values indicate how different the characteristics of ferritic cores may be from metallic ones. They are for Ferramic 34-A a product of the General Ceramics and Steatite Corp. The comparison is made against regular Deltamax and is quite extreme.

Material	Deltamax	Ferramic 34-A
Max. differential ~~incremental~~ permeability, $\mu_{\delta i}$, gausses/oersted	1.3×10^6	about 10^3
Coercive force, H_c, oersteds	0.06	3.5
Saturation flux density, B_s gausses	1.6×10^4	1.3×10^3
Volume resistivity at room temp., ρ, ohm-cm	under 10^{-4}	10^9

Figure 24a, below, is a photograph of scope traces showing the output pulses from a small Ferramic 34-A F109 toroidal core with a near-square cross-section of about 0.2-inch on edge. The applied H_e was asymmetrical, so that the pulses shown resulted from returning along a path very close to the saturation loop.

Figure 24b shows the reduction in response times resulting from symmetrical excitation, as discussed for metallic cores.

Figure 24c, when compared with Figure 24a, shows the reduction in response times resulting from reducing the radial thickness of a Ferramic 34-A F109 toroid to about $\frac{1}{2}$ its original value.

In the three figures a very reduced <u>range</u> of response-time values is evident. This reduction is largely due to the now finite rise time of the H_e function; the no longer negligible rise time effectively puts a lower limit on the response times of the ferritic cores for $H_e \gg H_2$. The fact that the toroids have relatively large radial thicknesses also contributes to this effect, and reduces the accuracy of any response-time correlations.

The resistivity of the Ferramic core is about 10^{13} times that of Deltamax. It is sufficiently high so that macroscopic eddy currents have been reduced to a negligible value and response times are of the same order of magnitude as the rise and fall times of the H_e pulses and of the associated circuitry. It is also possible that displacement currents and residual losses are significant limiting factors in this area.

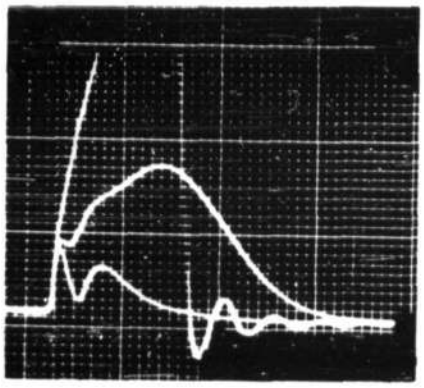

(a) FAMILY OF OUTPUT PULSES (FOR THREE H_e AMPLITUDES) FOR FERRAMIC 34-A F109 UNDER ASYMMETRICAL EXCITATION.

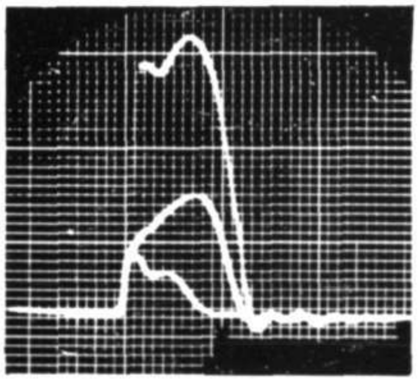

(b) FAMILY OF OUTPUT PULSES (FOR THREE H_e AMPLITUDES) FOR FERRAMIC 34-A F109 UNDER SYMMETRICAL EXCITATION.

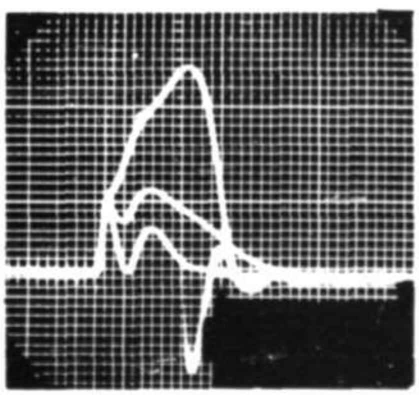

(c) FAMILY OF OUTPUT PULSES (FOR FOUR H_e AMPLITUDES) FOR FERRAMIC 34-A F109, WITH RADIAL THICKNESS HALVED, UNDER ASYMMETRICAL EXCITATION.

$\frac{1}{2}\,\mu$sec

A-3591 F-1106

FIG. 24

CHAPTER III

INFORMATION-RETENTION AND SIGNAL RATIOS

The operation of a magnetic core as described in Section B of Chapter I raises special problems with respect to stability of operation and what would commonly be called signal-to-noise ratios. In the first section of this chapter, these problems are discussed, and important ratios and criteria are set up and defined. There follows a brief look at the test setup used for obtaining the experimental results. These results, presented in the form of photographs and numerical values, are then discussed and related to hysteresis-loop shapes.

A. Definitions and Requirements

Much of the discussion below revolves around the voltage output pulses from a core for different situations and different core-information states. The measure of these output pulses may be taken as their areas, peak amplitudes, or amplitudes at chosen points in time. Unless otherwise stated, the pulse areas are taken to be the quantities under discussion. Polarities are often disregarded; it is assumed that, in the final system, the sensing device may be equally sensitive to signals of either polarity.

Reference should be made to Figures 1,2 (Chapter I) throughout this section.

1. <u>Information Retention</u>

This phrase is used to refer to the ability of a core to maintain a flux direction and magnitude, representing a ZERO or a ONE, <u>in the face of excitation by non-selecting ($H_M/2$) pulses</u>. Figure 1b shows how, after putting the core into state $-B_R$ with a full H_M pulse, a pulse of $H_M/2$ moves the core to a new state, $-B_N$. Additional applications of $H_M/2$ pulses tend to run the state of the core further up along the B axis, disturbing the information in the core, or, perhaps, destroying that information. An intuitive inference to be drawn from Figure 1b is that disturbance of the state of a core is reduced when the portion of the B-H loop between $H = -H_M/2$ and $H = +H_M/2$ approaches the horizontal. The degree to which that portion of the loop is horizontal is one of the measures of what is called loop rectangularity.

The state of a core is manifested by the size and shape of the voltage pulse out of a sensing coil in response to the read pulse of H. Change in amplitude or area of this output pulse as a function of the number of intervening non-selecting ($H_M/2$) pulses is, then, an indication of the sensitivity of a core to disturbance.

If a ONE, as written by a $-H_M$ write-ONE pulse, is at $-B_R$, and ZERO, as written by a $+H_M$ write-ZERO pulse, is at $+B_R$, then reading may be accomplished by applying a $+H_M$ read pulse, and the result is a large output voltage pulse for a ONE and a small output pulse for a ZERO.

Non-selecting read or write-ZERO pulses will tend to run a ONE position up along the B axis thus reducing the response to a read pulse later; they will not, however, significantly affect the ZERO position. On the other hand, non-selecting write-ONE pulses will tend to run a ZERO position down along the B axis thus increasing the response to a read pulse later; they will not, however, significantly affect the ONE position.

a. ONE-Retention

An "undisturbed ONE" is defined as the information state of a core after a ONE has been written and before any other pulses of H have been applied. A "disturbed ONE" is the state of a core when a very large number of non-selecting ($H_M/2$) read or write-ZERO pulses have followed the write-ONE pulse.

The "ONE-retention ratio" is defined as the ratio of output signals for the two cases:

$$\frac{\text{Disturbed ONE}}{\text{Undisturbed ONE}} \equiv \text{ONE-retention ratio, } R_1 .$$

R_1 approaches 1 in value for the ideal case and is less than 1 in practice.

b. ZERO-Retention

An "undisturbed ZERO" is defined as the information state of a core after a ZERO has been written and before any other pulses of H have been applied. A "disturbed ZERO" is the state of a core when a very large number of non-selecting ($-H_M/2$) write-ONE pulses have followed the write-ZERO pulse. The ZERO-retention ratio is defined as the ratio of output signals for the two cases:

$$\frac{\text{Disturbed ZERO}}{\text{Undisturbed ZERO}} = \text{ZERO-retention ratio, } R_0.$$

It approaches 1 in value for the ideal case and is greater than 1 in practice.

2. <u>Signal Ratios</u>

A number of signal ratios may be made from the above-mentioned four basic quantities. The most meaningful one is the "disturbed-signal ratio", which is defined as the ratio of output signals for a disturbed ONE and a disturbed ZERO, as follows:

$$\frac{\text{Disturbed ONE}}{\text{Disturbed ZERO}} = \text{Disturbed-signal ratio, } S_D.$$

Since disturbance generally reduces the output signal from a core with a ONE, and raises the output signal from a core with a ZERO, the S_D ratio is a really critical criterion of a core's performance. S_D approaches infinity in the ideal case, and approaches or falls below 1 for the unsatisfactory case. In practice it should be much greater than 1 if reasonable discrimination between the binary digits is to be obtained.

Another type of voltage output from a core occurs when it receives a non-selecting ($H_M/2$) pulse. This signal is, like noise, undesirable; the word noise is reserved, however, for signals which are more commonly described by that name, such as those resulting from inductive or capacitive pick up, etc. The first-mentioned signals will be called non-selecting (abbreviated N-S) signals.

The largest N-S signal from a core should occur in response to the first non-selecting ($H_M/2$) pulse of a polarity which tends to reduce the magnitude of the retained flux. If the core holds a ONE this would be a non-selecting read or write-ZERO pulse ($+H_M/2$).

The ratio of a disturbed-ONE signal to an N-S signal is defined as follows:

$$\frac{\text{Disturbed ONE}}{\text{N-S signal}} = \text{N-S signal ratio, } S_{ns}.$$

This ratio, like S_D, approaches infinity ideally, should be much greater than 1 for satisfactory operation, and is an important criterion of coincident-current core performance.

The garden variety of noise is not considered here; it will be one of the major problems involved in the development of assemblies of these cores into large-scale memories.

B. Test Setup

A single-pulse, or push-button, type of arrangement was first used in the experimental work. It was abandoned in favor of an automatic test setup which can put a repetitive pattern of H pulses on a core to simulate, approximately, some of the conditions under which the core might operate in practice. This setup makes it very easy to adjust the significant H amplitudes during operation and to see and record the output pulses from a test core for different operating modes.

Previous considerations lead directly to the pulse patterns desired for the testing. These are shown in Figure 25. The sequence of events for each mode of operation a, b, c, or d, may be followed with the aid of Figure 4b (Chapter I).

The block diagram of Figure 26 and the circuit schematic for the Core-Testing Pulse Amplifier (Figure 27) show the equipment arrangement and circuitry used to produce the above pulse patterns of magnetizing force.

The setup is very flexible and is made up largely of blocks of project test equipment.[7] Repetition rate may be varied by varying the free-running frequency of the high-frequency multivibrator in the MV Frequency Divider. All pulses are equal in duration; the duration may be varied by adjusting the delay in time between the pulse into and the pulse out of G & D (Gate and Delay) Unit 2. Pulse amplitudes are adjusted by front panel controls on the Core-Testing Pulse Amplifier. The modes of operation and the number of inserted non-selecting pulses are determined by the condition of the two switches,

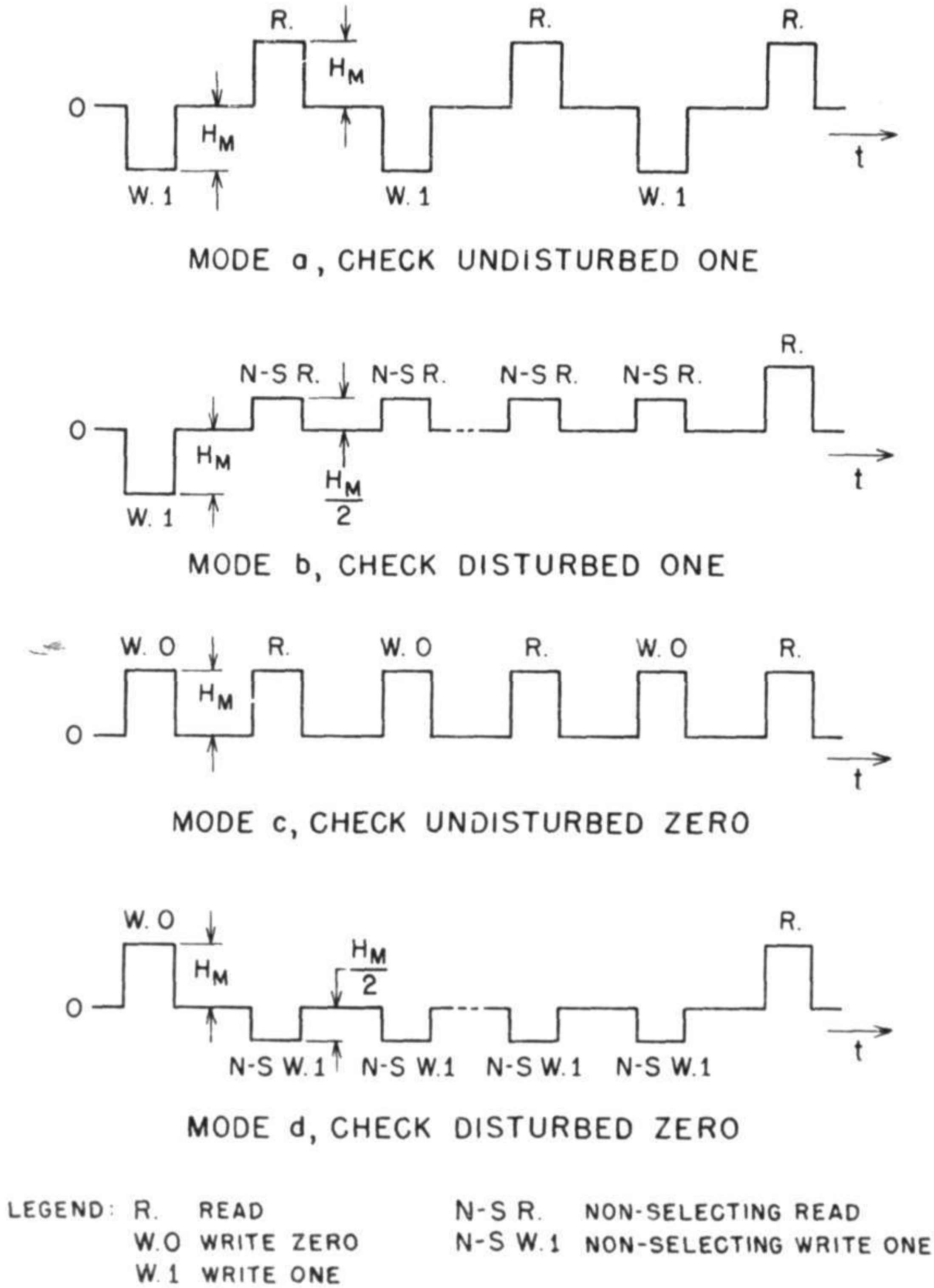

CORE-TESTING PULSE PATTERNS OF H

A-35973

FIG. 25

A-35972

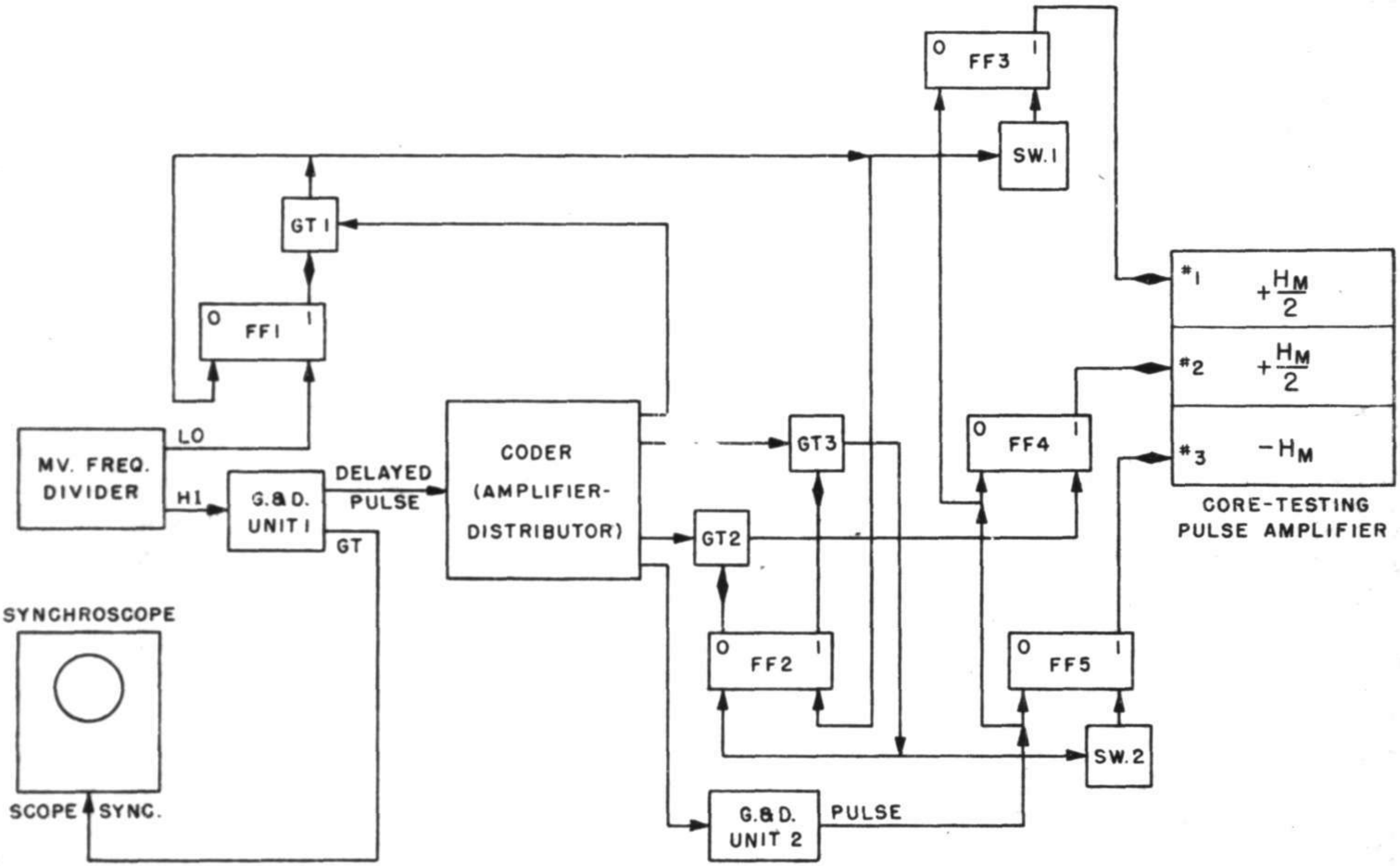

BLOCK DIAGRAM CORE-TESTING SETUP

FIG. 26

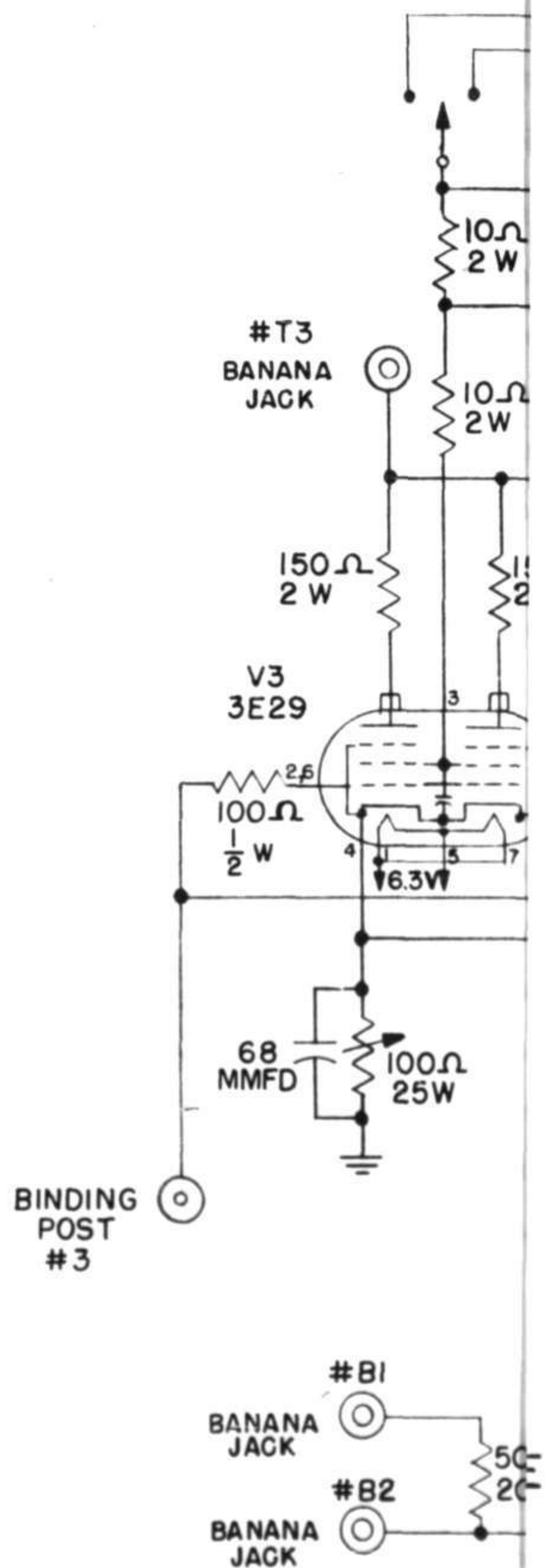

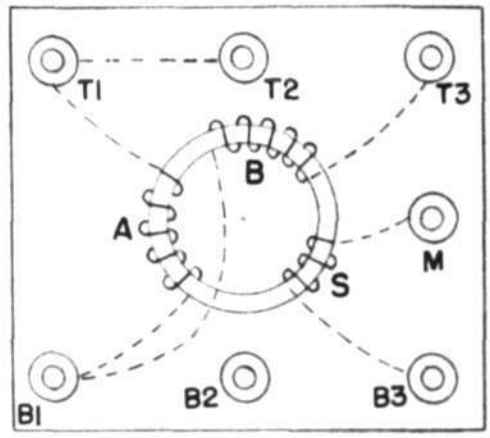

FRONT VIEW OF PLUG (OR PANEL)

E-TESTING PULSE
AMPLIFIER

FIG. 27

B-35929

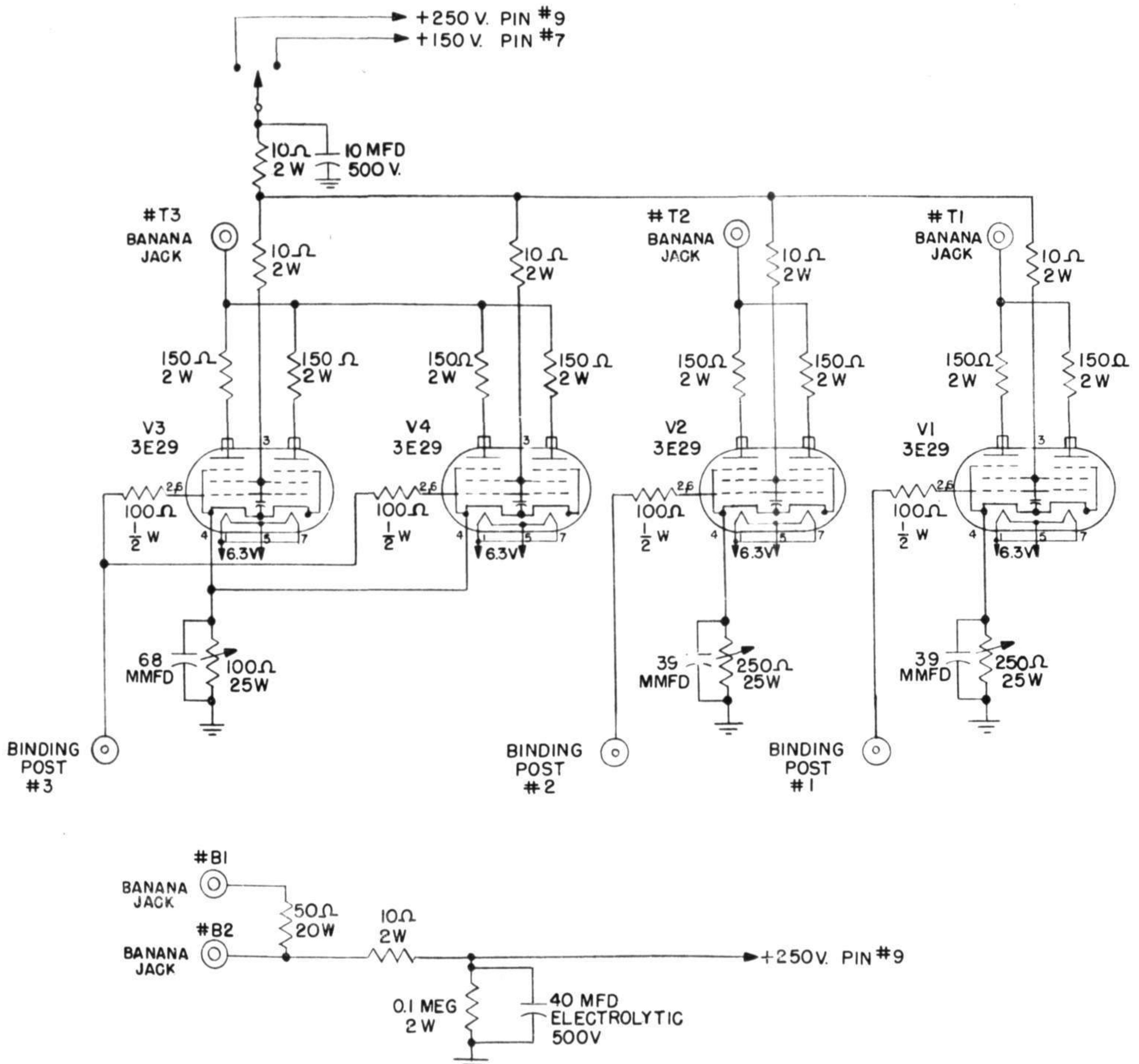

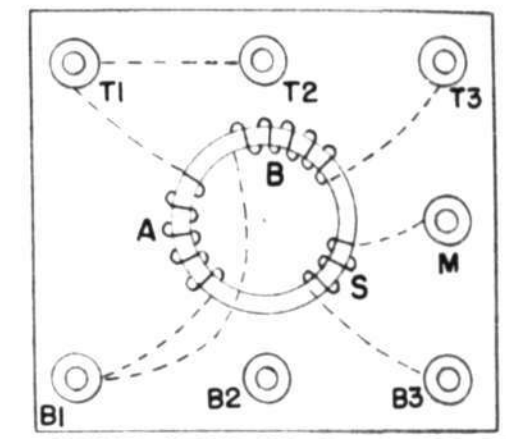

FRONT VIEW OF PLUG (OR PANEL)

CORE-TESTING PULSE AMPLIFIER

FIG. 2

SW 1 and SW 2, and the dividing ratio of HI- to LO-frequency pulses out of the MV Frequency Divider, as detailed below.

With the sync input of the synchroscope connected to receive the gate output of G & D Unit 1, as shown, it sweeps once for every pulse, regardless of operating mode. All output pulses start, therefore, at the same point on the scope screen (a point determined by the delay time of the pulse out of G & D Unit 1), and the viewed traces are superimposed. Scope leads may be connected to the sensing coil on a core for viewing output pulses, or across the 50-Ω, 20 w, series resistor which is common to the two magnetizing windings, for viewing the current pulses.

To produce operating mode a (Figure 25), the MV Frequency Divider (Figure 26) is adjusted to divide by 2, so that the repetition rate for "LO" frequency pulses is half that for "HI"; mode b is produced by dividing by any integer larger than 2. Opening switch SW 2 and dividing by 2 results in mode c. Mode d may be obtained by opening SW 1 and dividing by an integer greater than 2; the pattern will, however, by upside down and must be interpreted that way unless the trouble is taken to reverse either the magnetizing coil leads or the scope leads as was done in obtaining some of the disturbed-zero photographs of the next section.

C. <u>Experimental Results</u>

Few cores were found which could operate successfully in the coincident-current scheme. Of the metallic ones, core MTS 4382 (first mentioned in the previous chapter) was the best on all counts.

1. Core MTS 4382.

The test results for this core are summarized in the photographs of Figure 28 and the table of Figure 29.

Figure 28 is worth a considerable amount of study. The three columns of photographs are for three arbitrary values of H_M; the center column was taken with the magnitude of H_M close to the optimum value; the two side columns show the changes occurring for smaller and larger values. In the top row are shown the voltage drops across the series resistor common to both magnetizing coils; the scale is calibrated in oersteds since the voltage drop, multiplied by a known constant, gives the magnetizing force, H; these pictures, although taken for mode b, indicate the magnitudes of H_M and $H_M/2$ for the entire column.

The next four rows show the voltage pulses appearing on the core's sensing coil as the core reacts to the pulses of H.

Some jitter in the MV Frequency Divider between division by 2 and division by 3 made it possible to see the undisturbed-ONE output trace <u>and</u> the once-disturbed-ONE output trace simultaneously. This is labeled mode ab and is shown in the second row of the figure. The three positive traces (starting with the largest one) represent outputs from an undisturbed ONE, a once-disturbed ONE, and one non-selecting read pulse, respectively. The negative trace results from the write-ONE act.

A-36005 F-1107

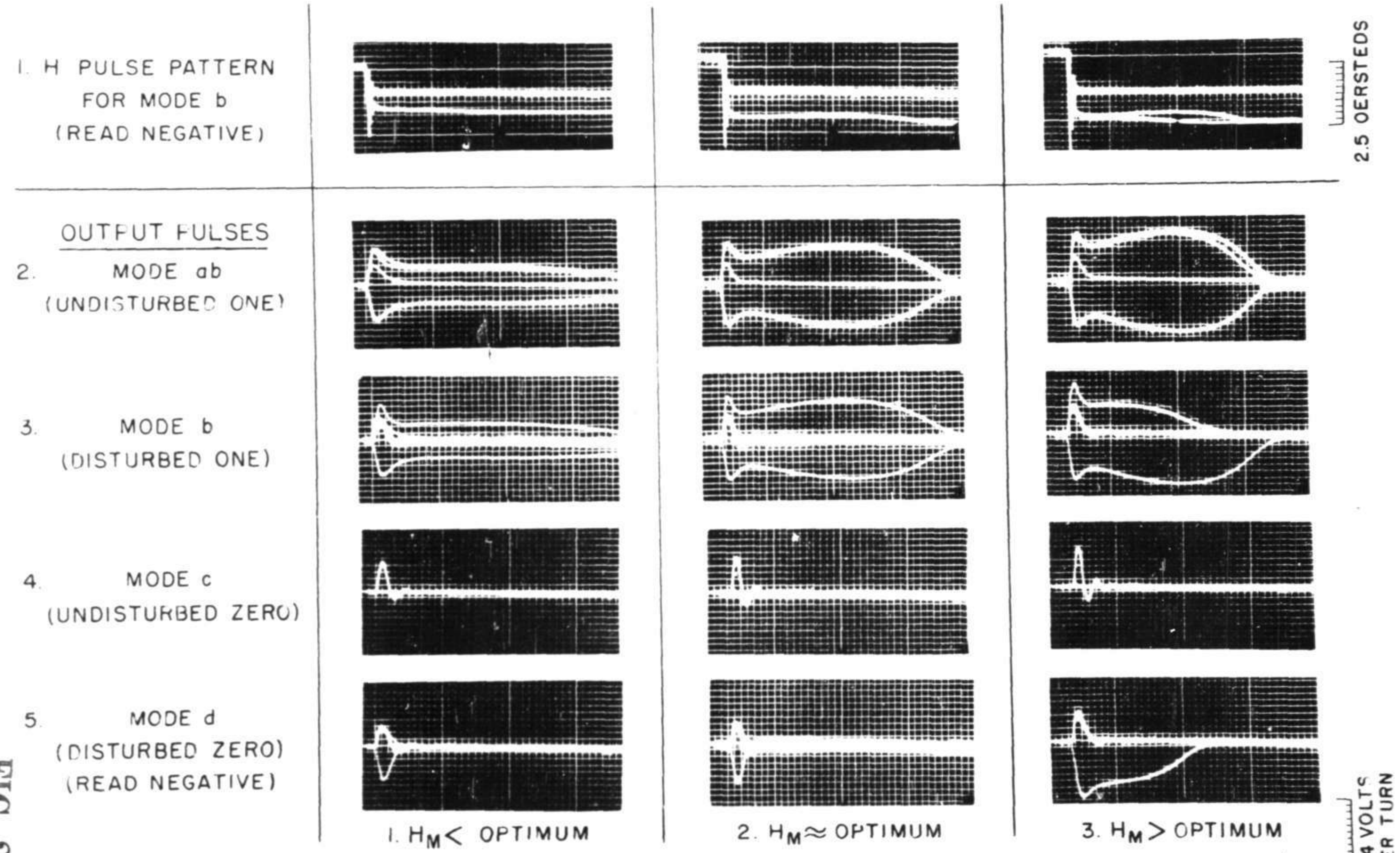

FIG. 28

COINCIDENT-CURRENT TEST RESULTS, METALLIC CORE MTS 4382

The third row shows mode b. The heavy center trace results from a large number of consecutive non-selecting read pulses; the finer trace just above it is from the very first of those. The positive outside trace represents the disturbed-ONE output, and the negative trace, as before, is from the write-ONE act.

Row 4, mode c, shows only one trace for the undisturbed ZERO.

Mode d, row 5, shows three traces. The negative trace represents the disturbed ZERO; the heavy positive trace results from the non-selecting write-ONE pulses; the faint positive trace results from the first one of the non-selecting write-ONE pulses.

The first table in Figure 29 shows approximate information-retention and signal ratios as obtained from the photographs. The results for columns 1 and 2 ($H_M \leq$ optimum) are most acceptable. Increasing H_M to the optimum value results mainly in a reduced response time and higher signal output levels. The increase to column 3 ($H_M >$ optimum) reduces the response time and raises output levels again, but it also results in drastically reduced signal ratios, particularly S_D.

Reference to the hysteresis loop (Figure 19) for this core shows that the $H_M/2$ value (1.5 oersteds) of column 3 exceeds the value (1.2 oersteds) of Figure 19, and is about equal to the H_c of the material. In column 2, however, $H_M/2 \approx 1.2 \leq H_1$, giving satisfactory operation.

A-36004

RATIO	OUTPUT SIGNAL	METALLIC CORE MTS 4382 $H_M <$ OPTIMUM	$H_M \approx$ OPTIMUM	$H_M >$ OPTIMUM
R_1	AREA RATIO	0.95	0.95	0.50
	AMPLITUDES AT 5 µsec	0.97	0.97	0.63
R_O	AREA	1.5	1.7	18
	5 µsec	1.0	1.0	$\rightarrow \infty$
S_D	AREA	10	13	0.80
	5 µsec	$\rightarrow \infty$	$\rightarrow \infty$	0.70
S_{ns}	AREA	12	16	8
	5 µsec	$\rightarrow \infty$	$\rightarrow \infty$	$\rightarrow \infty$
RESPONSE TIME		25 µsec	20 µsec	15 µsec

RATIO	OUTPUT SIGNAL	FERRITIC CORE 34A F109 (b.o.) $H_M <$ OPTIMUM	$H_M \approx$ OPTIMUM	$H_M >$ OPTIMUM
R_1	AREA RATIO	0.83	0.77	0.56
	AMPLITUDES AT 0.3 µsec	0.93	0.85	0.40
R_O	AREA	NOT TAKEN		
	0.3 µsec			
S_D	AREA	5.1	6.2	1.1
	0.3 µsec	2.5	13	1.1
S_{ns}	AREA	3.0	3.5	1.3
	0.3 µsec	10	7	1.6
RESPONSE TIME		0.45 µsec	0.45 µsec	0.6 µsec

FIG. 29

INFORMATION RETENTION AND SIGNAL RATIOS
FOR THE BEST METALLIC AND FERRITIC CORES

Comparison of Figure 19 with the family of B-H characteristics photographed in Figure 30a shows that the core retains its rectangularity well as H excursions are reduced, until some point is reached below which the loops collapse almost entirely. The predominant characteristics of the loop collapse are the large reductions in retained flux density, B_R. These reductions are greater, percentage-wise, than the concomitant reductions in coercive force, H_c. Although the ~~incremental~~ differential permeabilities decrease too, the overall effect is to maintain a loop shape on which the coincident-current criterion, $H_M/2 < H_1$ holds until the loops begin to collapse entirely. Also held well is the flatness of the near-horizontal portions of the loops, thus retaining favorable N-S signal ratios (S_{ns}).

2. <u>Core Ferramic 34-A F109 (b.o.)</u>

This is the best ferritic core tested and has reasonably acceptable retention and signal ratios plus an extremely short response time. It is, however, rather sensitive to the H_M amplitudes applied, and allows less deviation from the optimum H_M than does the metallic core previously discussed.

Figure 31 has photographs of the magnetizing pulses and the output pulses for the three important modes of operation. Scope leads were reversed when taking the photos of the H pulses and the mode d output pulses, so that all pertinent traces appear as positive ones. Otherwise interpretation is the same as for Figure 28.

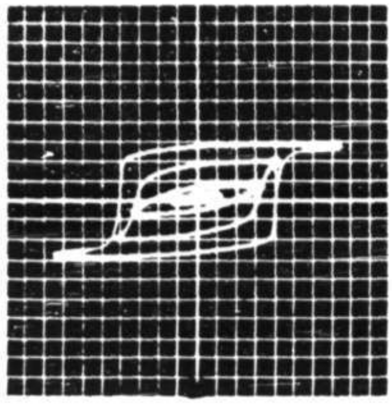

(a) FAMILY OF B-H CHARACTERISTICS FOR
METALLIC CORE MTS 4382

FERRAMIC 34, TYPE A

(b) SATURATION HYSTERESIS LOOP FOR
FERRITIC CORE FERRAMIC 34A AS
PUBLISHED BY THE MANUFACTURER

A-3606 F-1110

FIG. 30

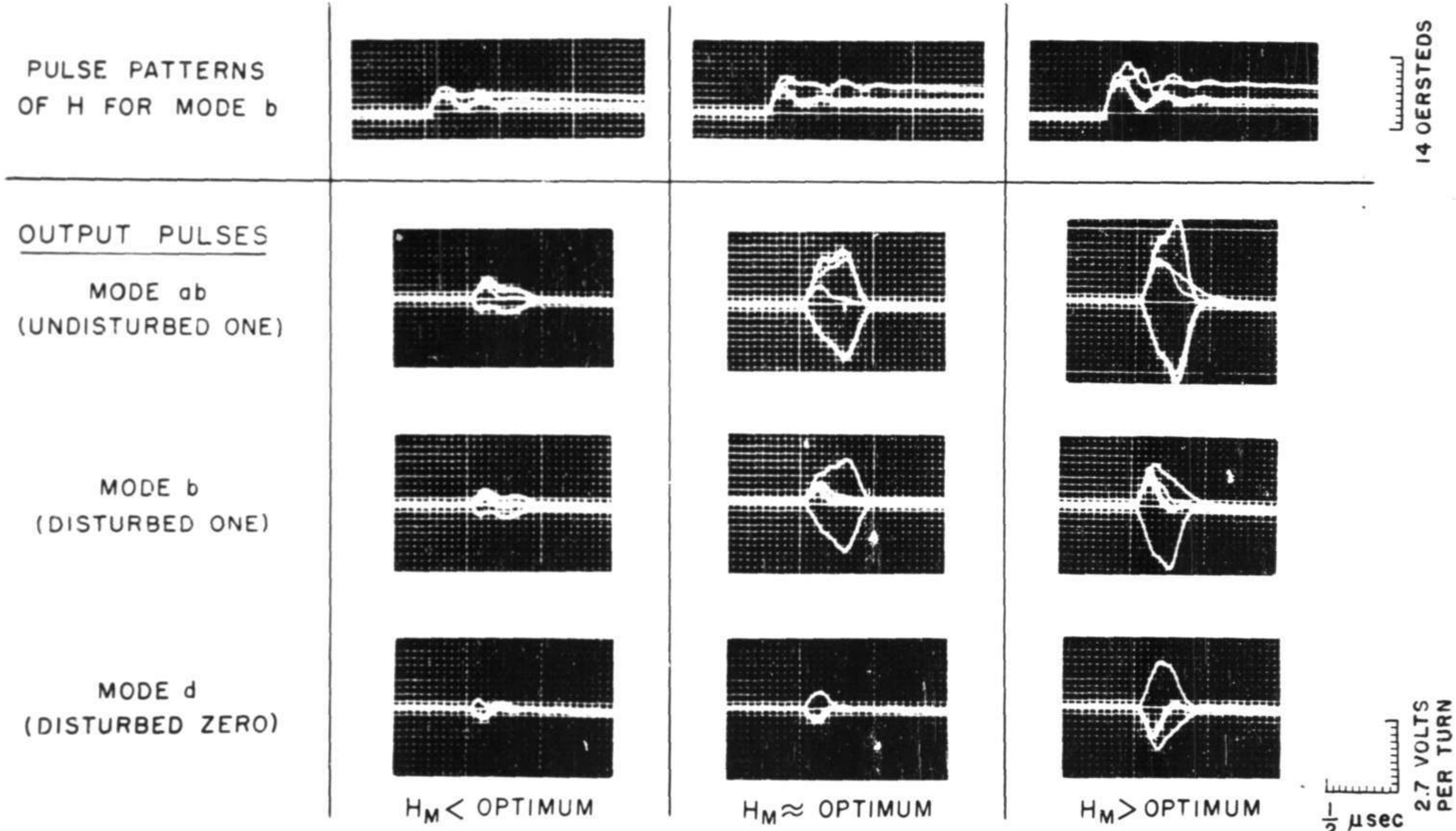

Fig. 31

COINCIDENT-CURRENT TEST RESULTS, FERRITIC CORE 34A F109 (b.o.)

The resultant important ratios are tabulated in Figure 29 next to those for core MTS 4382. The ferritic core has a response time about one-fortieth that for the metallic core, but it has appreciably poorer retention and signal ratios.

The response time improvement is largely due to the terrific reduction in eddy currents. The relatively poor signal ratios are due largely to a lower degree of hysteresis-loop rectangularity; a copy of a hysteresis loop for Ferramic 34-A is shown in Figure 30b.

Both the response-time values and the signal ratios at an optimum point in time could probably be improved somewhat by decreasing the rise times of the pulses of H.

3. Ferroxcube IV

An interesting demonstration of the effect of different degrees of hysteresis-loop rectangularity upon a core's performance may be had by rigging a negatively magnetostrictive core with a compression drawstrap and checking its performance, and its B-H characteristics, under varying degrees of compression.

This was done with a toroidal sample of Ferroxcube IV as supplied by the North American Philips Co. The photographs of Figure 32 show that core's performance when under a good amount of compression and when under none. The emergence of a fair degree of loop rectangularity under core compression may be seen in the upper two photographs.

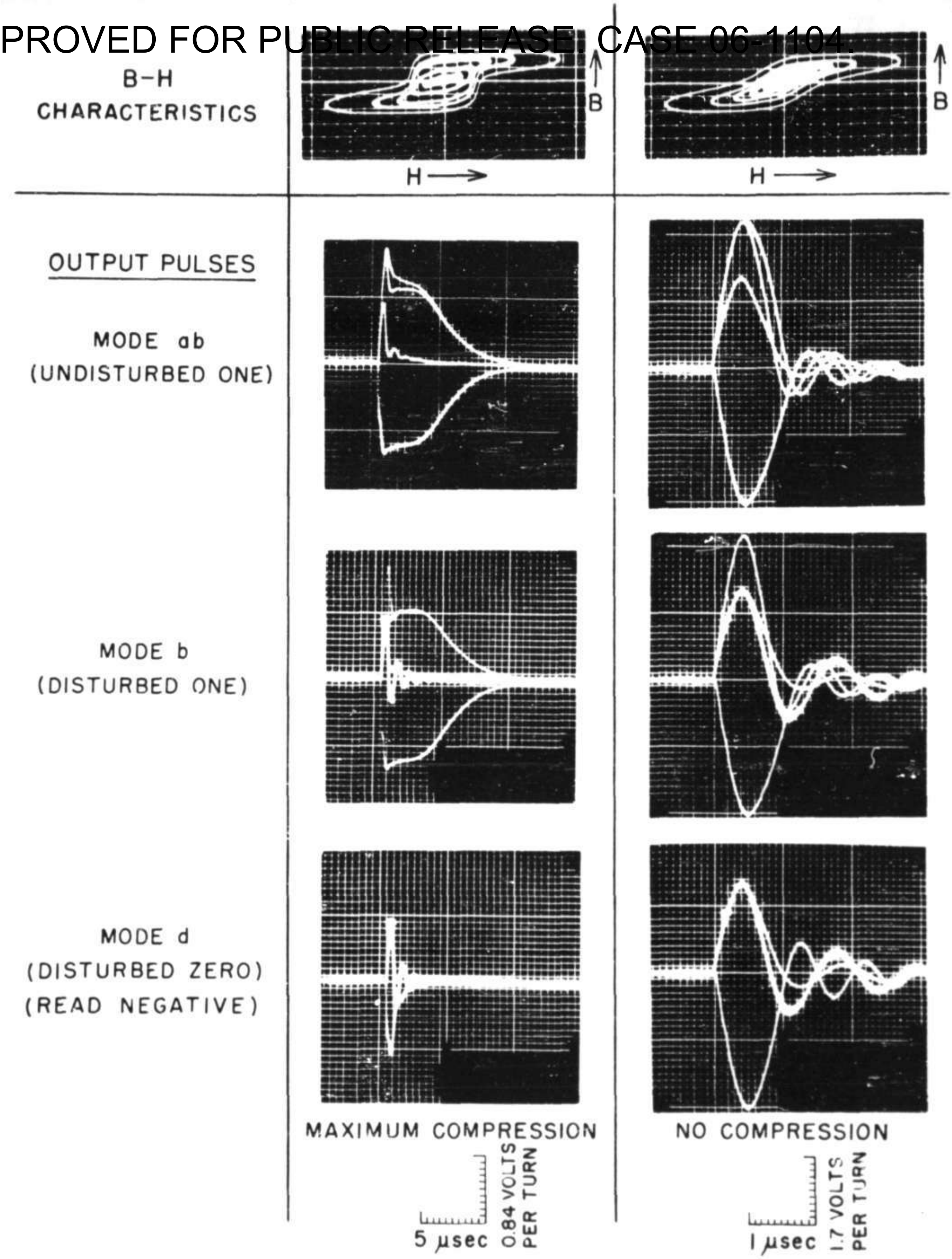

B-H CHARACTERISTICS AND COINCIDENT-CURRENT TEST RESULTS FOR A FERROXCUBE IV CORE UNDER DRAWSTRAP COMPRESSION

FIG. 32

A-360C F-1109

Along with the appearance of loop rectangularity under compression is the ability of the core to perform, with reasonable retention and signal ratios, in the coincident-current scheme. The core, when under no compression, has completely unacceptable ratios, as shown in the second column of the figure.

The response time of the core increases by a factor of about 10 when under compression. This is very roughly equal to the increase in the maximum ~~incremental~~ differential permeability (μ_{di}) with compression, as approximated from the middle loops of the two B-H characteristics shown. This is further evidence in support of some of the discussion in the preceding chapter.

Life-size photographs of the cores are displayed on the next two pages. Figure 33 shows pictures of the following: core MTS 4450, cased and wound (top left); a small-size, cased, sample core which has characteristics like MTS 4382 (top center); the Ferroxcube IV core with compression drawstrap and windings (top right); a regular Deltamax core, cased and wound (bottom left); a 1-mil Deltamax core out of its case (bottom right). Figure 34 shows cores MTS 4382 (left) and Ferramic 34-A F109 (b.o.) (right). Both cores are wound and mounted on a male plug of the Core-Testing Pulse Amplifier as used during the tests.

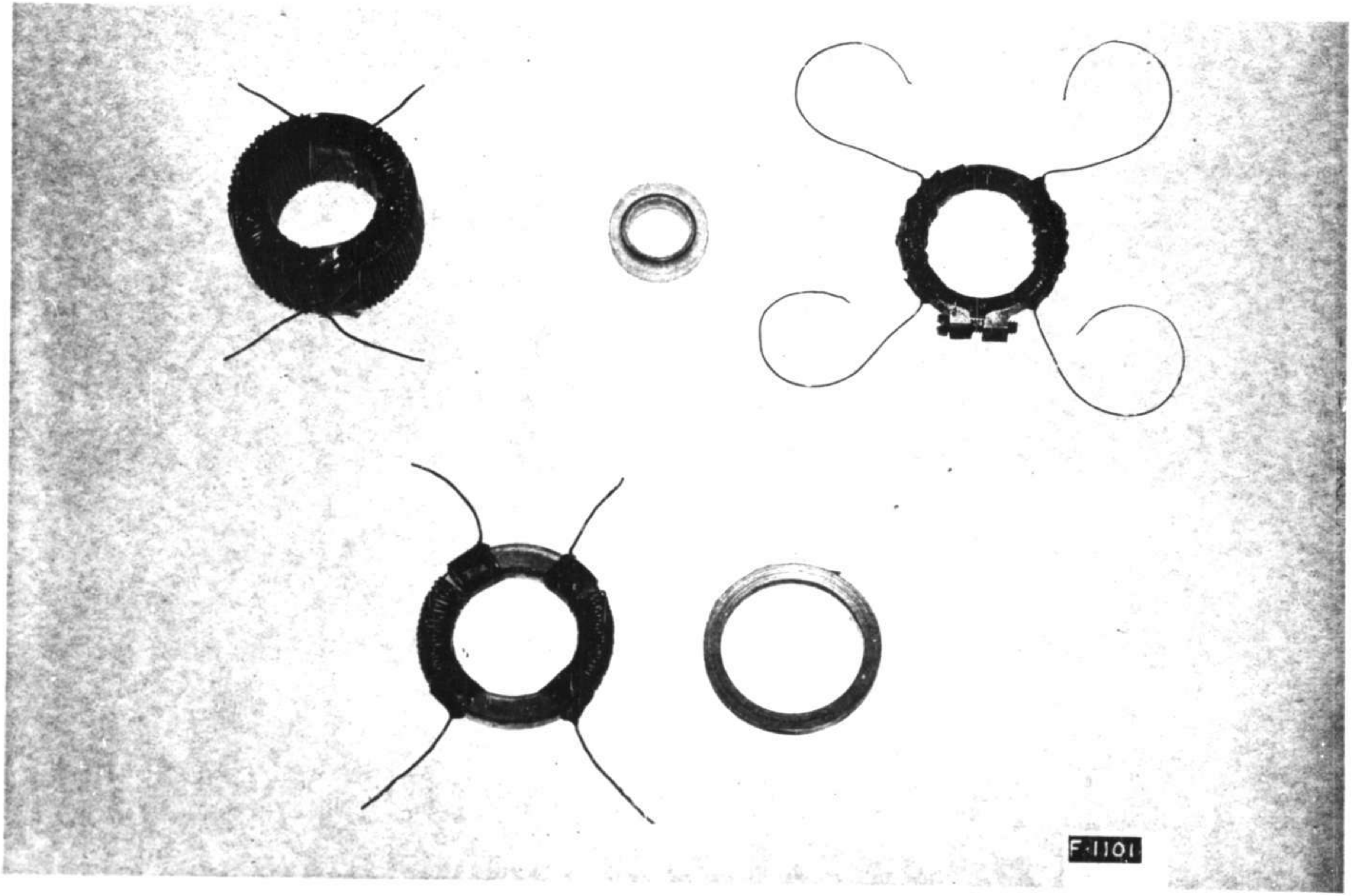

FIG. 33

LIFE-SIZE PHOTOGRAPHS OF SOME OF THE CORES

A-36011

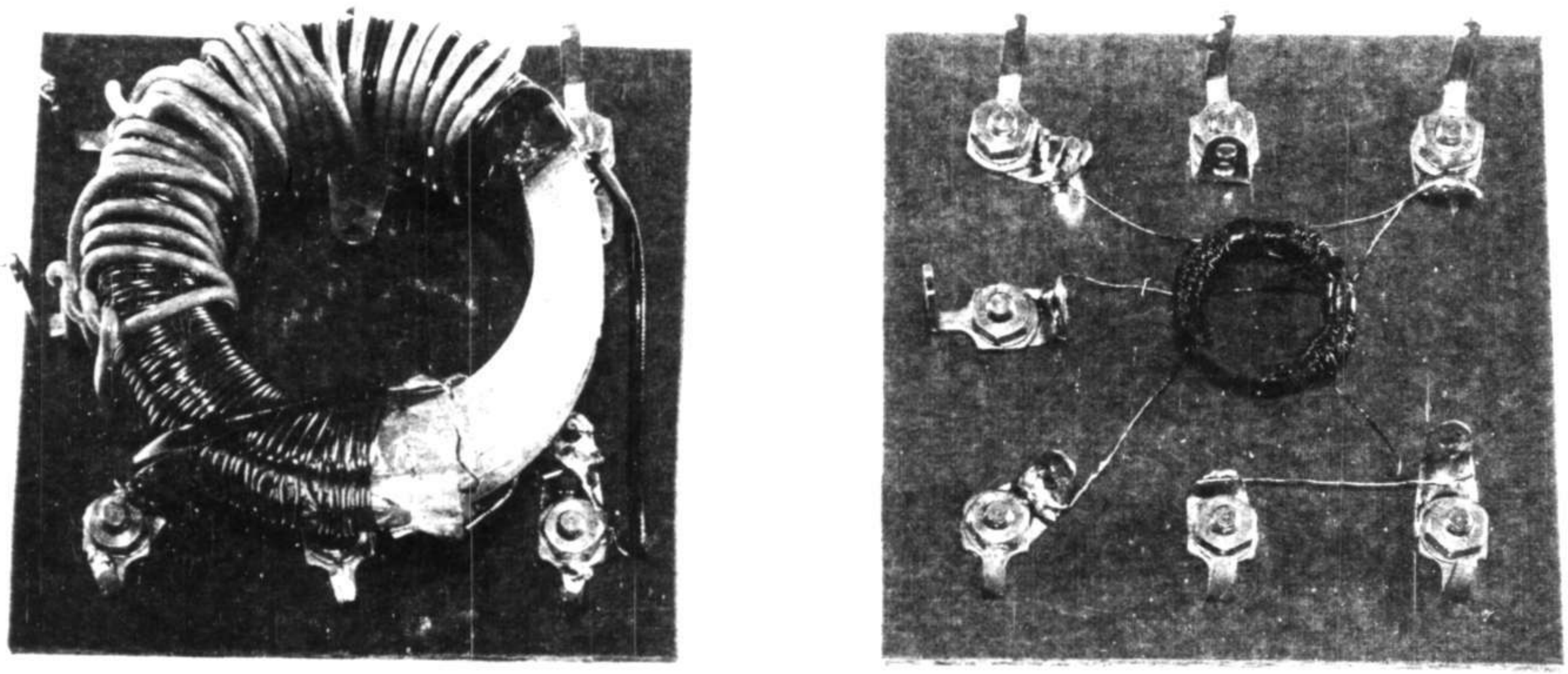

F·1102

FIG. 34

LIFE-SIZE PHOTOGRAPHS OF CORES MTS 4382 AND FERRAMIC 34A F109(b.o.) AS MOUNTED ON CORE TESTING PLUGS READY FOR USE IN THE TEST SETUP

CHAPTER IV

CONCLUSION

The preceding two chapters have dwelt on two phases of the problem of operating magnetic cores in a coincident-current memory scheme which would be adaptable to a line-switching type of selection along two or three space coordinates.

A. Response Times

The best response times presently attainable run to about 20 microseconds for metallic cores and about 1/2 microsecond for ferritic cores. The latter time is more than low enough by the high-speed-memory standards of Whirlwind I. Some decrease in response times is possible if the radial thickness of the ferritic toroids is reduced; further improvement may be attainable by changing material characteristics such as the volume resistivity.

The 20-microseconds response time of the best metallic core is too great for high-speed memory application in Whirlwind I, but is probably reasonable for intermediate applications and for slower computers. Very significant decreases in this core's response time are possible by reducing tape thickness (the Allegheny Ludlum Steel Corp. is working toward 1/4-mil tape - this should reduce response times to well below 5 microseconds), increasing material resistivity, and reducing the retained flux density.

B. Signal Ratios

Core MTS 4382 has probably as good a set of information-retention and signal ratios as will be needed in a coincident-current scheme which involves no more than three currents. The area ratios are extremely good, and the optimum-point-in-time ratios are practically perfect. These are all the result of a B-H characteristic which combines sharp corners, abrupt saturation, and the fact that H_1 and H_2 are close to each other yet relatively far from the origin, so that it is easy to find an H_M which fulfills the criterion, $H_2 < 2H_1$.

$\cancel{2H_1 > H_M > H_2.}$

C. Core B-H Characteristics

The operation of a core as a coincident-current memory unit requires a high degree of hysteresis-loop rectangularity. It also requires that the hysteresis loops of the core collapse toward the origin, for decreasing excursions of H, in a certain way. Future data on magnetic cores for this type of application should be in the form of families of B-H curves, or hysteresis loops, taken for symmetrical excitation values which range from zero to near saturation, with emphasis on the region about H_c. A family of such curves, supplemented by physical data regarding dimensions, resistivity, Curie temperature, etc., will convey about all the information needed in order to assess the core's suitability. There is quite a resemblance between such data and more commonly seen vacuum-tube data.

D. Miscellaneous Considerations

There are some phases of the problem which have been omitted or only lightly mentioned so far.

One of these is the fact that reading the core's information is the same as writing a zero into it. The core, in other words, is cleared upon being read. This is not a major impediment to the scheme's usefulness in a large-scale computer; it is not too difficult to re-write information extracted from a memory register. Thought should be given, however, to means of circumventing this problem.

The energy irreversibly put into a core during the switching process is quite significant. The required power may be a problem to supply and to dissipate as heat from the cores.

The average power into core MTS 4382 during the 20 microseconds switching time is of the order of 10 watts. If the core is operated at a 50% duty cycle (a reversal every 40 microseconds) it has to dissipate about 5 watts without experiencing a dangerous temperature rise. Since this core is fairly large (see Figure 34) and has a high Curie temperature, it can probably operate under these conditions fairly well, and the problem may only be that of removing the combined heat generated in an assembly of such cores. Under the same duty cycle of 50% (a reversal every microsecond) core Ferramic 34-A F109 (b.o.) may have to dissipate about 10 watts. This core is already rather small, and it has a relatively low Curie temperature (280°C). Unless special precautions are taken, this core's temperature may rise, during operation, to a point where its hysteresis-loop shape is adversely affected.

The energy into the core is in the form of a current pulse against the induced back e.m.f. Production of the proper current pulses for a large number of cores may be a serious problem, particularly if the current magnitudes are kept high in order to reduce the number of turns needed on each magnetizing or selecting winding.

The signal-ratio problem may be acute in a large assembly of cores. Whether undesired signals (N-S signals and ZERO's) will add or cancel each other will depend on the sensing circuit arrangements. The timing of the selecting pulses also enters into whether or not N-S signals become objectionable.

There is a large, thin, spike at the beginning of each output pulse from those cores which have response times longer than about 5 microseconds. This spike may also be seen as the start of each $K \frac{d\phi}{dt}$ pulse on the theoretical approximations of Figures 11 and 13, where the H pulses are considered to be step functions. Where H pulses have rise times which are negligible fractions of the core response time, the spikes appear. It is obvious, then, that the actual shape of these magnetizing pulses is a critical factor which needs to be determined for each situation; and the spikes may be reduced as desired, at the expense of some slight increases in response times.

Inductive pickup may become a real headache and the proper use of unilateral impedance elements, careful relative placement of cores, and other precautions may be necessary.

 78

These and other miscellaneous considerations require further study and experiment. Particularly needed is the experimental operation of a few cores in a two-dimensional pilot assembly. This work will begin at Project Whirlwind in the near future.

Signed. William N. Papian
William N. Papian

Approved. JWF
Jay W. Forrester

WNP:ap

APPENDIX

DERIVATION: H inside a thin ribbon as a function of x and t.

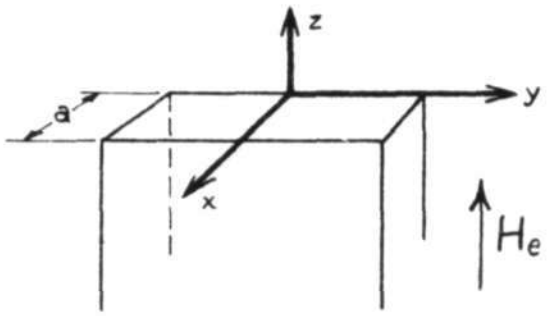

Thin ribbon of thickness a, infinite in z directions, "semi-infinite" in y directions; conductivity σ; step function of H, of amplitude H_e, applied at $t = 0$; $B = H = 0$ at $t = 0(-)$.

Maxwell's equations:

$$\nabla \times \vec{E} = -\frac{\partial \vec{B}}{\partial t}, \quad \nabla \times \vec{H} = \vec{i} + \frac{\partial \vec{D}}{\partial t}$$

Due to the assumed geometry, and disregarding displacement currents:

$$E_z = B_x = B_y = \frac{\partial \vec{E}}{\partial z} = \frac{\partial E_x}{\partial y} = 0,$$

$$H_x = H_y = i_z = \frac{\partial \vec{D}}{\partial z} = \frac{\partial \vec{H}}{\partial z} = \frac{\partial H_z}{\partial y} = 0,$$

leaving:

$$\frac{\partial E_y}{\partial x} = -\frac{\partial B_z}{\partial t} \quad \text{and} \quad \frac{\partial H_z}{\partial x} = -i_y.$$

Substituting $E_y = \frac{i_y}{\sigma}$

gives:

$$\frac{\partial i_y}{\partial x} = -\sigma \frac{\partial B_z}{\partial t} \quad \text{and} \quad \frac{\partial H_z}{\partial x} = -i_y.$$

Differentiating the second equation w/r to x, manipulating, combining, and dropping subscripts results in:

$$\frac{\partial^2 H}{\partial x^2} - \sigma \frac{\partial B}{\partial t} = 0 \qquad (1)$$

When B is a single-valued, linear, function of H, we may define a constant, called the permeability, as:

$$\mu \equiv \frac{B}{H} ,$$

in which case eq. 1 becomes:

$$\frac{\partial^2 H}{\partial x^2} - \sigma \mu \frac{\partial H}{\partial t} = 0 \qquad (2)$$

The solution for this equation follows a similar one that starts on page 189 of reference 8.

Boundary and initial conditions are:

$$H(0,t) = H(a,t) = H_e;\ H(x,0) = 0.$$

Say that:

$$H = H_S + H_T = \text{Steady state sol'n + transient sol'n.}$$

H_S satisfies one particular sol'n of eq. 2:

$$H_S = H_e$$

To find the transient part of the sol'n we set up new boundary conditions:

$$H_T\ (0,t) = H(0,t) - H_S = H_e - H_e = 0, \tag{3}$$

$$H_T\ (a,t) = H(a,t) - H_S = H_e - H_e = 0. \tag{4}$$

Another particular sol'n of eq. 2 is:

$$H = (c_3 \sin bx + c_4 \cos bx)\ e^{-\frac{b^2 t}{\sigma\mu}} \tag{5}$$

Substituting eq. 3 into eq. 5:

$$H_T\ (0,t) = (c_3 \sin 0 + c_4 \cos 0)\ e^{-\frac{b^2 t}{\sigma\mu}} = 0$$

$$\therefore\ c_4 = 0, \text{ and}$$

$$H_T = c_3 \sin bx\ e^{-\frac{b^2 t}{\sigma\mu}} \tag{6}$$

Substituting eq. 4 into eq. 6:

$$H_T\ (a,t) = c_3 \sin ba\ e^{-\frac{b^2 t}{\sigma\mu}} = 0$$

$$\therefore\ \sin ba = 0, \text{ and } b = \frac{n\pi}{a}\ ,$$

so that:

$$H_T = \sum_{n=0}^{\infty} C_n \sin \frac{n\pi}{a} x\ e^{-\frac{n^2\pi^2 t}{\sigma a^2 \mu}} \tag{7}$$

New initial conditions are:

$$H_T(x,0) = H(x,0) - H_S = 0 - H_e = -H_e.$$

Substituting these into eq. 7:

$$H_T(x,0) = \sum_{n=0}^{\infty} C_n \sin \frac{n\pi}{a} x = -H_e.$$

$$\therefore C_n = -\frac{2H_e}{n\pi}(1 - \cos n\pi) = -\frac{4H_e}{n\pi}, \text{ for odd n.}$$

So that:

$$H_T = -\sum_{n=1}^{\infty} \frac{4H_e}{n\pi} \sin \frac{n\pi x}{a} e^{-\frac{n^2\pi^2 t}{a^2\sigma\mu}}, \qquad (8)$$

And:

$$H = H_e\left(1 - \frac{4}{\pi} \sum_{n=1}^{\infty} \frac{1}{n} \sin \frac{n\pi x}{a} e^{-\frac{n^2\pi^2 t}{a^2\sigma\mu}}\right), \text{ odd n.} \qquad (9)$$

— — —

REFERENCE BIBLIOGRAPHY

1. Jay W. Forrester, "Digital Information Storage in Three Dimensions Using Magnetic Cores," Project Whirlwind Report R-187, (May 16, 1950), M.I.T. Servomechanisms Laboratory.

2. Jay W. Forrester, "Data Storage in Three Dimensions," Project Whirlwind Memorandum M-70, (April 29, 1947), M.I.T. Servomechanisms Laboratory.

3. Harvard University Computation Laboratory, Progress Reports 2-6 (August 1948 - November 1949), Investigations for Design of Digital Calculating Machinery, (particularly No. 2, part IV).

4. J. L. Snoek, New Developments in Ferromagnetic Materials, (New York: Elsevier Publishing Co., 1947).

5. Brockman, Dowling, and Steneck, "Dimensional Effects Resulting from a High Dielectric Constant Found in a Ferromagnetic Ferrite," The Physical Review, 77,1 (Jan. 1950).

6. R. M. Bozorth, "Magnetism," Review of Modern Physics, 19 (Jan. 1947).

7. R. R. Rathbone, "Specifications for Standard Test Equipment," Project Whirlwind Report R-143, (Jan. 18, 1949), M.I.T. Servomechanisms Laboratory.

8. P. Franklin, Differential Equations for Electrical Engineers (New York: John Wiley & Sons, Inc., 1933).